https://doi.org/10.5194/egusphere-2024-952
Preprint. Discussion started: 19 April 2024

Assessing the global contribution of marine, terrestrial bioaerosols, and desert dust to ice-nucleating particle concentrations

Marios Chatziparaschos[1,2,*], Stelios Myriokefalitakis[3], Nikos Kalivitis[1], Nikos Daskalakis[4], Athanasios Nenes[2,5], María Gonçalves Ageitos[6,7], Montserrat Costa-Surós[6], Carlos Pérez García-Pando[6,8], Mihalis Vrekoussis[4,9,10] and Maria Kanakidou[1,2,4]

[1]Environmental Chemical Processes Laboratory (ECPL), Department of Chemistry, University of Crete, Heraklion
[2]Center for the Study of Air Quality and Climate Change (C-STACC), Institute of Chemical Engineering Sciences (ICE-HT), Foundation for Research and Technology, Hellas) (FORTH), Patras, Greece
[3]Institute for Environmental Research and Sustainable Development, National Observatory of Athens (NOA), GR-15236 Palea Penteli, Greece
[4]Laboratory for Modelling and Observation of the Earth System (LAMOS), Institute of Environmental Physics (IUP), University of Bremen, Bremen, Germany
[5]Laboratory of Atmospheric Processes and their Impacts (LAPI), School of Architecture, Civil and Environmental Engineering (ENAC), Ecole Polytechnique Federale de Lausanne, Lausanne, Switzerland
[6]Barcelona Supercomputing Center (BSC), Barcelona, Spain
[7]Department of Project and Construction Engineering, Universitat Politècnica de Catalunya (UPC), Barcelona, Spain
[8]Catalan Institution for Research and Advanced Studies (ICREA), Barcelona, Spain
[9]Center of Marine Environmental Sciences (MARUM), University of Bremen, Germany
[10]Climate and Atmosphere Research Center (CARE-C), The Cyprus Institute, Nicosia, Cyprus
*Now at Barcelona Supercomputing Center (BSC), Barcelona, Spain

Correspondence: Maria Kanakidou (mariak@uoc.gr)

Abstract. Aerosol-cloud interactions, and particularly ice crystals in mixed-phase clouds (MPC), stand as a key source of uncertainty in climate change assessments. State-of-the-art laboratory-based parameterizations were introduced into a global chemistry-transport model to investigate the contribution of mineral dust, marine primary organic aerosol (MPOA), and terrestrial primary biological aerosol particles (PBAP) to ice nucleating particles (INP) in MPC. INP originating from PBAP (INP_{PBAP}) are found to be the primary source of INP at low altitudes between -10ºC and -20ºC, particularly in the tropics, with a pronounced peak in the Northern Hemisphere (NH) during boreal summer. INP_{PBAP} contributes about 27% (in the NH) and 30% (in the SH) of the INP population. Dust-derived INP (INP_D) show a prominent presence at high altitudes in all seasons, dominating at temperatures below -25°C, constituting 68% of the INP average column burden. MPOA-derived INP (INP_{MPOA}) dominate in the Southern Hemisphere (SH), particularly at subpolar and polar latitudes at low altitudes for temperatures below -16ºC, representing approximately 46% of INP population in the SH. When evaluated against available global observational INP data, the model achieves its highest predictability across all temperature ranges when both INP_D and INP_{MPOA} are included. The additional introduction of INP_{PBAP} slightly reduces model skills for temperatures lower than -16ºC; however, INP_{PBAP} are the main contributors to warm-temperature ice nucleation events. Therefore, consideration of dust and marine and terrestrial bioaerosol as INP precursors is required to simulate ice nucleation in climate models. In this respect, emissions, ice-nucleating activity of each particle type and its evolution during atmospheric transport require further investigations.

https://doi.org/10.5194/egusphere-2024-952
Preprint. Discussion started: 19 April 2024

1 Introduction

Cloud ice exerts a multifaceted influence on climate (Zhang et al., 2020), affecting the radiative balance (Zhou et al., 2016; Yi, 2022), climate feedback mechanisms (e.g., temperature, albedo, water vapor feedbacks) (Choi et al., 2014), precipitation patterns (Sorooshian et al., 2009), and climate sensitivity (Murray et al., 2021). In mixed-phase clouds, ice particles and cloud droplets coexist in an unstable thermodynamic equilibrium owing to subzero temperatures. A significant feature of MPC is the degree of homogeneity of mixing ice particles and liquid droplets (Korolev and Milbrandt, 2022). These clouds are prevalent throughout the troposphere, observed across all latitudes, spanning from polar regions to the tropics (D'Alessandro et al., 2019). As a result, they significantly impact precipitation rates and the radiative energy balance on both regional and global scales.

Within MPC, the interaction between ice particles and liquid droplets occurs through the molecular diffusion of water vapor. Ice particles can grow at the expense of evaporating cloud droplets when the ambient water vapor pressure lies between the saturation water vapor pressure with respect to ice ($e_{s,i}$) and water ($e_{s,w}$). This case, known as the Wegener-Bergeron-Findeisen (WBF) process, is caused by the difference in supersaturation between the liquid and ice phases (Pruppacher et al., 1998), with the latter being consistently lower. Other factors that alter saturation water vapor pressure can be the vertical velocity as a source for water vapor, and the integrated ice crystal surface which depletes supersaturation by consuming the available water vapor (Korolev, 2007). For the WBF process to occur, ice formation is first required, following two formation pathways: via homogeneous freezing at temperatures lower than −38 ◦C (Liu et al., 2012) or heterogeneous freezing at warmer temperatures (Murray et al., 2012), with the latter being crucial for ice formation in MPC. The presence of aerosols is necessary for heterogenous freezing since they provide a surface for the ice to form on. These aerosols called ice nucleating particles (INP), a select subgroup of aerosol particles - approximately 1 in 10^5 particles in continental air are activated at -30°C (DeMott et al., 2010) - that initiate ice formation heterogeneously (Vali et al., 2015). Once the first ice crystals are formed, triggered by INP, they can rapidly grow via the WBF process and multiply via secondary ice processes (Georgakaki et al., 2022; Korolev and Leisner, 2020), affecting precipitation ranges, cloud properties, and albedo.

The simulation of ice crystal concentrations in climate models is therefore important for determining the properties of MPCs, and uncertainties in the INP levels can lead to discrepancies in the modelled top-of-atmosphere radiative flux, and estimates of climate sensitivity to greenhouse gases (Vergara-Temprado et al., 2018; Murray et al., 2021). With climate change, and considering temperature changes alone, liquid water may progressively replace ice in MPC of a given altitude, making them more reflective. However, the magnitude of this so-called cloud-phase feedback is highly uncertain (Frey and Kay, 2018), partly due to uncertainties in the present and future spatiotemporal distribution of INP (Zhao et al., 2021; Hoose et al., 2010; Raman et al., 2023) and the structure of layered cloud systems that would promote glaciation through the seeder-feeder mechanism (Ramelli et al., 2021). The inability of models to represent the occurrence frequency and glaciation state of MPC is also hypothesized as a major reason making climate models (Bodas-Salcedo et al., 2016) and reanalysis products (Naud et al., 2014) disagree with each other in the annual mean downward solar (short-wave, SW) radiation.

https://doi.org/10.5194/egusphere-2024-952
Preprint. Discussion started: 19 April 2024

INP can originate from a number of sources, each with its own set of characteristics and properties. In the absence of a well-established theory for heterogeneous ice nucleation, INP prediction typically relies on empirical parameterizations that are subject to considerable uncertainty and challenges. Advancing the predictability of INP abundance with reasonable spatiotemporal resolution will require an increased focus on research that bridges the measurement and modeling communities. Additionally, coupling cloud processes to simulated aerosol also makes cloud physics simulations increasingly susceptible to uncertainties in simulation of INP, due to the lack of sufficient observational constraints.

Many substances have been shown to nucleate ice, depending on the cloud type and the predominant freezing mechanisms. Reviewing experimental and modeling studies, Burrows et al. (2022) summarized the level of understanding and parameterisations of INP activity of 10 particle types that could represent INP in climate models. In immersion freezing, which is the dominant mode of primary ice formation in MPC (Hande and Hoose, 2017), desert dust, marine primary organic aerosols (MPOA) and terrestrial primary biological aerosol particles (PBAP) have emerged as the most relevant INP sources (McCluskey et al., 2018; Chatziparaschos et al., 2023; Spracklen and Heald, 2014; Cornwell et al., 2023). These findings align with the physical understanding that INP are often efficiently activated as cloud condensation nuclei due to internal mixing with soluble components and their large size. These particles are likely enclosed within cloud droplets, making them available for immersion freezing but unavailable for contact freezing. The latter is constrained by the collision rate between interstitial particles and supercooled liquid droplets, a process that remains poorly understood at a fundamental level in real clouds (Kanji et al., 2017). Consequently, the role of contact freezing and its contribution to primary ice formation in MPC is characterized by high uncertainty.

Globally, airborne mineral dust from deserts and other drylands is considered the dominant INP source at temperatures below -20°C (Murray et al., 2012; Kanji et al., 2017). For instance, Pratt et al. (2009) identified that ~50% of the ice crystal residual particles sampled in clouds at high altitudes over Wyoming were mineral dust. Studies have subsequently demonstrated that dust mineralogy plays a pivotal role in influencing the ice-nucleating efficiencies of mineral dust (Atkinson et al., 2013; Boose et al., 2016, 2019; Cziczo et al., 2013; Hoose et al., 2008), with several studies finding potassium enriched (K-) feldspar to be the most INP active dust mineral (Atkinson et al., 2013; Augustin-Bauditz et al., 2014; Zolles et al., 2015; Peckhaus et al., 2016; Harrison et al., 2019; Holden et al., 2019). Additionally, quartz is a major component of airborne mineral dust (Glaccum and Prospero, 1980; Perlwitz et al., 2015a, b) and exhibits a strong INP activity (Atkinson et al., 2013; Zolles et al., 2015; Losey et al., 2018; Kumar et al., 2019b; Holden et al., 2019). Quartz particles have substantially lower INP efficiencies than K-feldspar particles (Harrison et al., 2019), but their much higher abundance in the atmosphere can lead to an important INP contributor (Chatziparaschos et al., 2023). Nevertheless, there are other minerals present in the atmosphere, such as smectite (Kumar et al., 2023) and kaolinite (Wex et al., 2014) but their contribution to INP levels remains unknown. Some laboratory studies have found that organic-rich soil dust from agricultural lands is more INP active than inorganic desert dust (Suski et al., 2018), although this fraction is typically not represented in climate models (Burrows et al. 2022).

While it is well established that dust particles are the most abundant source of INP at temperatures below -20°C, it is equally well established that terrestrial bioaerosol or PBAP, such as fungal spores, bacteria,

https://doi.org/10.5194/egusphere-2024-952
Preprint. Discussion started: 19 April 2024

pollen, and plant debris, are highly efficient ice nucleators at warm temperatures (Huang et al., 2021; Cornwell et al., 2022) and may have a substantial effect on ice crystal formation (Prenni et al., 2009). Only a small fraction of biological material can trigger ice nucleation (Huang et al., 2021), with INP concentrations estimated at approximately 1 to 2 per liter (Pöschl et al., 2010). Although these INP levels are much lower than usually observed for warm MPC, ice crystal formation from PBAP can be subsequently enhanced by ice multiplication processes ("secondary ice") (Korolev and Leisner, 2020) which are most efficient at temperatures warmer than -15°C (Georgakaki et al., 2022; Sullivan et al., 2018). Recent advances in remote sensing and model/sensor fusion have enabled the presence of secondary ice in clouds, revealing that this process holds particular significance in temperatures ranging from -5°C to -20°C (Wieder et al., 2022; Billault-Roux et al., 2023). At the same time, the presence of SIP may actually mitigate uncertainties in INP predictions, given that ice crystal formation can be a self-limiting process (e.g., Sullivan et al., 2018).

Global simulations including biological particles have estimated that PBAP contribute to droplet freezing rates in the warm parts of mid-latitude clouds, with about 1×10^{-5} % of the global average ice nucleation rates, and an upper-most estimate of 0.6% (Hoose et al., 2010). Spracklen and Heald, (2014) suggest that PBAP can dominate immersion freezing rates at altitudes between 400 and 600 hPa, in agreement with observational studies (Pratt et al., 2009). Field measurements have observed enhancements in both PBAP and INP related to rainfall events (Huffman et al., 2013; Tobo et al., 2013; Mason et al., 2015; Kluska et al., 2020) and suggested that PBAP emissions are affected by relative humidity (Prenni et al., 2013). Tobo et al. (2013) found that in a mid-latitude ponderosa pine forest, the variation pattern of INP concentration was like that of fluorescent biological aerosol particles during summertime, suggesting that PBAP are critical contributors to INP. Consequently, PBAP acting as INP at warm freezing temperatures may be an important source of INP in regions where they are abundant and may have a noteworthy impact on climate. However, modelling of PBAP remains challenging due to the complexity of ecosystem processes and a lack of observations (Burrows et al., 2022).

Organic material with INP potential is also associated with sea spay aerosol (SS) emissions from the ocean. Historically, SS was considered unimportant as a source of atmospheric INP. However, recent observational and modelling studies have revealed that emitted MPOA mixed with SS is potentially an important or even the only source of INP of marine origin (Wilson et al., 2015; Mitts et al., 2021). McCluskey et al. (2018a, 2018b, 2019) confirmed that SS was strongly associated with MPOA as the primary organic INP source. Wilson et al. (2015) showed experimentally that marine organic material associated with phytoplankton and cell exudates in the sea surface microlayer is an important source of atmospheric INP. In an exploratory model study, Burrows et al. (2013) showed that marine biogenic INP are likely to significantly contribute to the concentration of INP in the near-surface air over the Southern Ocean. INP derived from MPOA have potentially a remarkable effect on solar radiation, cloud glaciation and precipitation at high and mid-latitudes in remote marine regions especially during winter (Wilson et al., 2015). Huang et al. (2018) found that marine INP had only a small effect on cloud ice number concentration and effective radius, and did not significantly affect the global radiative balance. However, they emphasized that the relative importance of MPOA as an INP was found to be significantly dependent on the type of ice nucleation parameterisation scheme that is chosen. Marine INP are not the main source of INP across all ocean areas. Gong et al. (2019) concluded that SS contributed less to the total INP in

https://doi.org/10.5194/egusphere-2024-952
Preprint. Discussion started: 19 April 2024

the atmosphere in Cape Verde than the other precursors of INP such as dust. In contrast, Vergara-Temprado et al. (2018) and McCluskey et al. (2019) proposed that MPOA are an important source of INP in remote marine environments. The largest concentrations of marine INP occur over the Southern Oceans, the North Atlantic and the North Pacific in regions where biological activity in surface ocean waters and wind speeds are greatest, while mineral dust from deserts (the major terrestrial INP source) only accounts for a small fraction of the observed INP in this region (Wilson et al., 2015; Huang et al., 2018).

In this study, we enhance our comprehension of the global spatiotemporal distribution of INP by incorporating both marine and terrestrial biogenic INP precursors, namely MPOA and PBAP, here encompassing bacteria and fungal spores, building upon our earlier investigation of mineral dust-derived INP (Chatziparaschos et al., 2023). The methodology involves utilizing a 3-dimensional chemistry transport model for conducting simulations. Heterogeneous nucleation in the immersion mode is parameterized based on the singular hypothesis (Vali et al., 2015), using aerosol-specific parameters derived from laboratory and field observations. Figure 1 presents a comprehensive schematic illustration of INP formation derived from mineral dust, MPOA and PBAP. We identify major sources of INP and the specific aerosol types capable of acting as INP, dependent on location and season. Additionally, we assess the relative contribution of bioaerosols to ice nucleation via immersion freezing in comparison to mineral dust and pinpoint regions and altitudes where this contribution holds significance. Simulated INP concentrations are rigorously evaluated against available INP observations sourced from the BACCHUS (Impact of Biogenic versus Anthropogenic emissions on Clouds and Climate: towards a Holistic Under Standing; http://www.bacchus-env.eu/) and Wex et al. (2019) databases.

2. **Methods**

2.1 Model description

The well-documented 3-dimensional global chemistry-transport model TM4-ECPL (Kanakidou et al., 2020; Myriokefalitakis et al., 2015, 2016) is used here, driven by ERA-Interim reanalysis (Dee et al., 2011) meteorological fields from the European Centre for Medium-Range Weather Forecasts (ECMWF). The model is run with a horizontal resolution of 3° longitude by 2° latitude with 25 hybrid pressure vertical levels from the surface up to 0.1hPa (~ 65 km) and a model time step of 30 min. The TM4-ECPL model considers lognormal aerosol distributions in fine and coarse modes and allows hygroscopic growth of particles, as well as removal by large-scale and convective precipitation and gravitational settling. Advection of the tracers in the model is parameterized using the slopes scheme (Russell and Lerner, 1981), and convective transport is parameterized based on Tiedtke (1989) and the Olivié et al. (2004) scheme. Vertical diffusion is parameterized as described in Louis (1979). For wet deposition, both large-scale and convective precipitation are considered. In-cloud and below-cloud scavenging are parameterized in TM4-ECPL, applied as described by Jeuken et al. (2001) and references therein. For all fine aerosol components, dry deposition is parameterized similarly to that of non-sea-salt sulfate, which follows Tsigaridis et al. (2006). Also, gravitational settling (Seinfeld and Pandis, 1998) is applied to all aerosol components.

https://doi.org/10.5194/egusphere-2024-952
Preprint. Discussion started: 19 April 2024

2.2 Atmospheric cycle of INP-relevant aerosols

Desert dust emissions are calculated online as described in Tegen et al. (2002) and implemented as in Van Noije et al. (2014). Following Chatziparaschos et al. (2023), we consider both K-feldspar and quartz as the INP active mineral species of dust, whose fractions in the soil-surface are taken from the global soil mineralogy atlas of Claquin et al. (1999), with updates provided in Nickovic et al. (2012). The calculation of the emitted mass fractions of K-feldspar and quartz in the accumulation and coarse modes [with dry mass median radii (lognormal standard deviation) of 0.34μm (1.59) and 1.75μm (2.00), respectively] is based on brittle fragmentation theory (Kok, 2011). Thus, the mass emission of each mineral is calculated by applying the respective mineral-emitted mass fractions to the dust emission fluxes. All minerals are emitted externally mixed, and dust particle density is equal to 2650 kg m^{-3} (Ginoux et al., 2004; Tegen et al., 2002). The modelled mineral dust mass concentration and deposition fluxes have been evaluated against global observations in a previous study (Chatziparaschos et al., 2023).

Terrestrial bacteria and fungal spores are the PBAP considered in this study. In light of the well-documented discrepancies in INP activity spanning several orders of magnitude between various bioaerosol types (Murray et al., 2012; Kanji et al., 2017), it appears imprudent to assume that any individual species is representative of ambient PBAP. Therefore, we use parameterizations based on concurrent measurements of INP together with broad classification of bioaerosol (bacteria, fungal spore) types (Tobo et al., 2013). Terrestrial bacteria (BCT) emissions are parameterized as proposed in Burrows et al. (2009b), where near-surface observations were used in combination with model simulations to determine the optimal BCT flux rates for particles with a diameter of 1 μm [monodisperse spherical particles], across six different ecosystems: coastal: 900; crops: 704; grassland: 648; land ice: 7.7; shrubs: 502; and wetlands: 196m^{-2} s^{-1}. For the present study, the Olson Global Ecosystem Database (Olson, 1992), originally available for 74 different land types on a spatial scale of 0.5◦×0.5◦, was grouped into 10 ecosystem groups as proposed by Burrows et al. (2009b). Consequently, the total bacteria flux is calculated as a sum of bacteria fluxes per ecosystem, weighted by the corresponding area of each ecosystem within the model's grid box. In TM4-ECPL, upon emission, the insoluble fraction of PBAP becomes progressively soluble due to atmospheric ageing. This process, which has been seen to occur, for instance, by degradation of RNA (Paytan et al., 2003) is parameterized based on oxidant levels as for all organic aerosols in the model (Tsigaridis and Kanakidou, 2003; Tsigaridis et al., 2006). Thus, the mean turnover of aged PBAP is estimated by applying a hydrophobic to hydrophilic conversion rate that depends on the atmospheric oxidants and is equivalent to a global mean turnover of 1.15 days (Tsigaridis and Kanakidou, 2003; Kanakidou et al., 2012). Regarding deposition, the hydrophilic aerosols are removed from the troposphere faster by dry and wet deposition than the hydrophobic ones.

Fungal spores (FNG) fluxes are treated as linearly dependent on the leaf area index (LAI) and the specific humidity based on a parameterization proposed by Hummel et al. (2015). This parameterization is informed by field measurements of fluorescent biological aerosol particles conducted at diverse locations across Europe. In the TM4-ECPL, the parameterization that is used to calculate FNG emissions online uses monthly averaged LAI distributions from the Global Land Cover 2000 database (European Commission, Joint Research Centre, 2003) as Hummel et al. (2015) and 3-hourly averaged specific humidity and temperature data, as provided by ERA-Interim. Bioaerosol sizes range from fine to coarse,

https://doi.org/10.5194/egusphere-2024-952
Preprint. Discussion started: 19 April 2024

but since their shapes are not accurately known, for the present work, FNG are assumed to be monodisperse spherical particles of 3 μm diameter with 1000 kg m^{-3} density (Hummel et al., 2015). The organic matter to organic carbon ratio (OM:OC) of all PBAP is set equal to 2.6, and the molecular weight equal to 31 g mol^{-1}, using mannitol as a model compound (Heald and Spracklen, 2009; Myriokefalitakis et al., 2016).

The role of pollen as INP has been demonstrated in previous studies (Hoose et al., 2010; Pummer et al., 2012); however, its experimental determination is challenging due to its large size and spatiotemporal variability. With a mean diameter ranging from 10 to 125 μm (Jacobson and Streets, 2009) models assume that pollen is emitted as entirely soluble aerosol (Hoose et al., 2010), resulting in substantial wet and dry deposition (Myriokefalitakis et al., 2017). Therefore, considering its size, pollen is anticipated to have much lower number concentrations compared to other PBAP at MPC altitudes, except possibly during periods of strong pollen emissions in the spring. However, pollen potentially impacts at low clouds as effective cloud condensation nuclei (Subba et al., 2023). Consequently, uncertainties in pollen emission, size distribution, hygroscopicity, and ice activity that varies among pollen species (Pummer et al., 2015), lead us not to consider pollen as INP in this study. Overall, a fundamental understanding of bioaerosol types and the mechanisms of their emission from the biosphere into the atmosphere is lacking, highlighting the need for process studies to build confidence in INP model extrapolations in a changing biosphere.

MPOA emissions are calculated online by the model considering the partitioning between insoluble marine organics and sea salt, as described in detail in Myriokefalitakis et al. (2010). The parameterization is based on O'Dowd et al. (2008), modified by Vignati et al. (2010). MPOA is calculated as a fraction of the submicron sea-salt aerosol based on chlorophyll-a (Chl-a) present in the ocean surface layer. The organic mass fraction is calculated as a linear relation to Chl-a, valid for Chl-a concentrations below 1.43 μg m^{-3} (for larger values, the percentage is kept constant at 0.76). Following sea-salt emission, MPOA is emitted, assuming that it is entirely insoluble, as determined by O'Dowd et al. (2008). The final MPOA diameter is dependent on Chl-a uptake (Vignati et al., 2010), scaling to a minimum diameter of 0.09 μm. Additionally, based on Facchini et al. (2008), we adopted a coarse mode MPOA source (Gong, 2003; Myriokefalitakis et al., 2010). The sea-salt source is calculated online by TM4-ECPL driven by wind speed at every time-step, following Gong (2003) and fitted for accumulation and coarse modes as described in Vignati et al. (2010). In TM4-ECPL, Chl-a concentrations are satellite-derived monthly average MODIS observations at a resolution of 1°x1°. The density of water-insoluble organic mass was set to 1000 kg m^{-3} (Vignati et al., 2010) and that of dry sea salt to 2165 kg m^{-3} (O'Dowd et al., 2008). The ageing of insoluble MPOA is taken into account, as for all other insoluble primary organic aerosols in the model, and corresponds to a global mean turnover time of about 1 day (Cooke et al., 1999; Tsigaridis and Kanakidou, 2007). Model results have been evaluated against observations in the marine environment by comparing water-insoluble organic carbon observations with modelled insoluble MPOA, as referred in Myriokefalitakis et al. (2010).

https://doi.org/10.5194/egusphere-2024-952
Preprint. Discussion started: 19 April 2024

2.3 Ice nucleation parameterizations

2.3.1. Desert dust: The effect of dust minerals on the INP concentration is parameterized using the singular approximation based on the laboratory-derived active site density parameterizations for K-feldspar and quartz minerals provided in Harrison et al. (2019). The parameterization for K-feldspar is valid in the temperature range between -3.5ºC and -37.5ºC, while for quartz, between -10.5ºC and -37.5ºC. To calculate aerosol surface area, we assume that each mineral dust particle is spherical and externally mixed (Atkinson et al., 2013; Vergara-Temprado et al., 2017). The density of ice nucleation active surface sites, derived from the spectrum of ice nucleation properties and for a polydisperse aerosol sample, is assumed to follow a Poisson distribution:

$$INP_D = \sum_i \sum_j n_{i,j} \left\{1 - e^{[-S_{i,j} n_{s(i)}(T)]}\right\} \quad \textit{Eq. 1}$$

where INP_D is the number concentration of ice formed on the mineral dust aerosol, $n_{i,j}$ is the total dust mineral particle number concentration (per m^{-3}), where index i corresponds to mineral type (quartz and K-feldspar) and index j to size mode (accumulation and coarse mode). $S_{i,j}$ is the individual dust particle mean surface area (cm^{-2}) in size mode j. Air temperature, T, is given in degrees Kelvin and $n_{s(i)}$ corresponds to the active site density of each mineral (Harrison et al., 2019). Further details on the methodology and the evaluation of the simulated INP derived from mineral dust are provided in Chatziparaschos et al. (2023).

2.3.2 PBAP: The number concentration of INP derived from PBAP is based on the parameterization of Tobo et al. (2013), which considers the dependence of INP on temperature and the number concentration of aerosol particles with diameters larger than 0.5μm. Particles with diameters above this threshold are assumed to have a sufficient surface area to provide active sites for ice nucleation (DeMott et al., 2010). Tobo et al. (2013) derived a parameterization of INP_{PBAP} from observations of INP and ambient fluorescent biological aerosol particles (FBAP) in a mid-latitude ponderosa pine forest ecosystem. They, thus, proposed to calculate INP_{PBAP} number concentration for temperatures ranging from about -9°C to -34°C and the number concentrations of FBAP, hereafter replaced by that of PBAP, as follows:

$$INP_{PBAPs} = \left(N_{PBAPs,>0.5\mu m}\right)^{\alpha'(273.16-T)+\beta'} e^{\gamma'(273.16-T)+\delta'} \quad \textit{Eq. 2}$$

where α' =-0.108, β' = 3.8, γ' = 0, and δ' = 4.605 and N_{PBAP} is the number concentration (m^{-3}) of PBAP (FNG and BCT) larger than 0.5μm, and T the air temperature in Kelvin. There are two limitations in using this parameterization. Firstly, this parameterization has been derived from a mid-latitude ponderosa pine forest ecosystem and therefore its application on a global scale remains a rough approximation. Secondly, FBAP may also contain non-PBAP (e.g., mineral dust particles, secondary organic aerosol particles) that contribute to fluorescence (Bones et al., 2010; Lee et al., 2013; Morrison et al., 2020). The number fractions of FBAP to the total aerosol particles in the super-micron size range could be relatively similar to those of PBAP under dry conditions (Tobo et al., 2013). However, during and after rain events,

https://doi.org/10.5194/egusphere-2024-952
Preprint. Discussion started: 19 April 2024

PBAP were underestimated by more than a factor of 2 (Huffman et al., 2013), suggesting that FBAP reflect only a portion of PBAP. Additionally, observations by Negron et al. (2020) suggest that airborne bacteria may be unambiguously detected with autofluorescence. Overall, there is ample evidence supporting a correlation between INP and total fluorescent particles (Huffman et al., 2013). However, the exact identity of these fluorescing particles has not yet been clarified adequately, and it remains challenging to determine better proxies for biological origin INP that can be readily measured in the environment.

***2.3.3 MPOA**:* The contribution of marine organic material to INP is parameterized according to Wilson et al. (2015), based on the total organic carbon (TOC) in the sea spray originating from the sea surface microlayer and the ice-nucleating temperature. It considers the active sites density per unit mass of TOC contained in insoluble MPOA and is derived from a spectrum of temperatures ranging from -6°C to -27°C. A factor of 1.9 is used for the conversion between MPOA and TOC in the model, as suggested in Burrows et al. (2013). The number concentration of INP_{MPOA} (m^{-3}) per TOC (g) originating from MPOA is calculated following the equation below.

$$INP_{MPOA} = C_{MPOA} e^{[11.2186-(0.4459*T)]} \quad Eq.\ 3$$

where C_{TOC} is the total organic carbon mass concentration (g/m^3) of marine particles and T is the air temperature in °C.

2.4 Simulations and INP evaluation

Simulations were performed from 2009 to 2016 using the year specific meteorological fields and emissions as described in the previous sections. The simulated INP are compared against the available INP observations from the databases of BACCHUS (http://www.bacchus-env.eu/in/index.php, last accessed on 26 March 2020) and Wex et al. (2019) (https://doi.pangaea.de/10.1594/PANGAEA.899701, last access on 14 February 2022). The observational data span from 2009 to 2016 and originate from different campaigns (locations are shown in supplementary Fig. S1). For this comparison, INP concentrations are calculated at the temperature at which the measurements were performed. All model results are compared to observations for the specific month and year of observation, except for those reported by Yin et al. (2012), which cover temporally scattered measurements (between 1963 and 2003) and are therefore compared to the modelled multi-annual monthly mean INP concentration from 2009 to 2016.

3 Results and Discussion

3.1 Global INP distributions

Figure 2 depicts annual zonal mean profiles of INP number concentrations that are derived from mineral dust, PBAP and MPOA (INP_D, INP_{PBAP}, and INP_{MPOA}, respectively) (Fig. 2a-c) along with their fractional contribution to the total INP concentration (Fig. 2d-f). INP_D (Fig. 2a) present considerable concentrations (>$5x10^{-1}$ L^{-1}) at temperatures colder than -20°C in agreement with findings by Hoose and Möhler (2012). Previous studies suggested that dust is the dominant source of immersion mode INP at temperatures

https://doi.org/10.5194/egusphere-2024-952
Preprint. Discussion started: 19 April 2024

colder than −25°C (Murray et al., 2012; Kanji et al., 2017). However, over the dust belt, dust has been found to initiate freezing in midlevel supercooled stratiform clouds at temperatures of −10°C and below (Liu et al., 2008; Zhang et al., 2012). These are warmer temperatures than those reported by Ansmann et al. (2008) who found no evidence of ice formation in supercooled stratiform clouds with cloud-top temperatures above −18°C, but colder temperatures than those found by Sassen et al. (2003), who attributed the glaciation of altocumulus clouds at −5°C to African dust. Although mineral dust can act as INP at warm temperatures, this depends on, among other factors, the amount of minerals [K-feldspar and quartz fraction (Chatziparaschos et al., 2023; Harrison et al., 2019)], particle size (Chen et al., 2021), particle concentration per droplet, and biological nanoscale fragments attached to dust particles (Augustin-Bauditz et al., 2016). Our model results show that PBAP are the primary source of INP between −12°C and −20°C. This agrees with a recent observational and modelling study by Cornwell et al. (2023). Overall, mineral dust (Fig. 2d) dominates INP levels at high altitudes almost over the globe in all seasons (Fig. S2). At intermediate pressure levels (up to 600hPa and T <-20 °C), INP_D dominate over the North Hemisphere (NH) (Chatziparaschos et al., 2023), where the major sources of dust minerals are located (Sahara, Gobi deserts and Arabian Peninsula). Between 20°S and 90°N, the simulated concentrations of INP are driven mostly by mineral dust and PBAP. MPOA plays a minor role, contributing less than 30% between 800 to 600 hPa (60 to 90°N).

INP_{PBAP} are important at low altitudes between 40°S and 90°N with concentrations >10 L^{-1} at -16°C. Their contribution to the total INP is more than 80% between -12°C to 16°C. PBAP are more ice-active than mineral dust at relatively high temperatures (Murray et al., 2012; Tobo et al., 2013; Harrison et al., 2019). INP_{PBAP} mainly affect the tropical and subtropical atmosphere during the whole year at temperatures higher than about -16°C over the SH and extend to pole in the NH. In boreal summer, due to vegetation growth, the INP_{PBAP} fractional contribution is shifted towards northern latitudes (Fig. 2S). Our results suggest that PBAP derived from forest biota play an important role in driving atmospheric INP concentrations both nearby and downwind of these ecosystems. They also show that PBAP may be the dominant precursor of INP at relatively warm temperatures, as has been previously suggested (Tobo et al., 2013; Murray et al., 2012; DeMott and Prenni, 2010). At temperatures colder than -20°C, nonbiological aerosol particles like mineral dust are effective INP (Murray et al., 2012; Si et al., 2019), thus dominating the INP population. In the NH, INP concentrations mainly originating from PBAP and mineral dust are higher than those in the SH where INP_{MPOA} dominates between 60°-90°S.

The simulated low INP_{MPOA} number concentrations (10^{-1} to $1L^{-1}$ at 800hPa, <-20°C) are consistent with the concentration range shown in Wilson et al. (2015) and Vergara-Temprado et al. (2018). Despite the relatively large sources of MPOA in the SH, a region covered mostly by sea, the resulting INP_{total} concentrations remain lower than those simulated over the NH, mostly continental, where dust and PBAP dominate. This pattern of low INP concentration in the SH agrees with observations in the Southern Ocean (Chubb et al., 2013) and could be translated into less cloud droplet freezing, enhancing cloud reflectivity (Vergara-Temprado et al., 2018). However, low INP concentrations could lead to the initial growth of large ice (i.e., in the seed region) and can influence the evolution of the microphysical cloud structure in the lower cloud levels (i.e., in the feeder region) enhancing precipitation (Borys et al., 2003; Ramelli et al., 2021). Significant radiation biases in the models occur mainly in remote marine regions away from major INP sources, where the prevalence of MPOA results in uniquely low INP

https://doi.org/10.5194/egusphere-2024-952
Preprint. Discussion started: 19 April 2024

concentrations (Vergara-Temprado et al., 2018). On a global scale, the small number of INP contributed by MPOA and the low sensitivity of cloud ice properties to ice nucleation, as suggested by Huang et al. (2018), imply that MPOA do not significantly affect the radiative balance. However, the relative importance of MPOA as an INP in the models depends strongly on the type of ice nucleation parameterisation scheme chosen (Huang et al., 2018). For instance, Vergara-Temprado et al. (2018) propose that the low INP_{MPOA} concentrations are essential to cloud reflectivity. They suggest that INP_{MPOA} are negatively correlated with shortwave (SW) radiation up to an INP concentration of 1 L^{-1}, above which the reflected radiation drops sharply as the ice processes become more efficient and deplete most of the liquid water. According to Huang et al. (2018), MPOA lead to a considerable increase in INP concentrations close to the surface in the polar regions as also here calculated and shown in figure 2c. Nevertheless, the impact of INP_{MPOA} is notably more pronounced in the SH, due to the increased competitiveness of INP_{PBAP} and INP_D concentrations in the NH. All in all, at high pressure levels, INP populations are influenced by the prevalence of bio-INP (INP_{MPOA} and INP_{PBAP}), with MPOA affecting INP concentrations mainly in the SH and PBAP in the NH.

Similar patterns emerge from the zonal mean seasonal analysis (Fig. S2). In the boreal winter and spring months (DJF, MAM), INP_D dominates at low pressure levels between 60°-90°N, with INP_{MPOA} contributing less than 30%. Meanwhile, between 60°S-60°N, INP_{PBAP} are prevalent but with low concentrations. INP_D remains the primary contributor to INP population at high altitudes, displaying a consistent pattern across all seasons. In JJA and SON, INP_{PBAP} and INP_{MPOA} dominate at low altitudes, showing alternating patterns influenced by vegetation and ocean biota. The recent observational study by Creamean et al. (2022) in the central Arctic revealed a strong seasonality of INP during the year, with lower concentrations in the winter and spring controlled by transport from lower latitudes, to enhanced concentrations of INP in the summer, likely from marine biological origin. This only partially agrees with our results showing that INP concentrations are influenced by transported airborne dust in winter, but INP_{PBAP} contribute more than INP_{MPOA} in summer. At warm temperatures (above -16 °C) in the Arctic, the majority of simulated INP are typically biological throughout the year. While at lower temperatures, INP are from continental sources (e.g. dust) and are mostly inorganic (INP_D).

Our findings highlight that INP at warm temperatures primarily derive from organic sources, as simulated by PBAP and MPOA. This biological contribution to INP at higher temperatures is important for subsequent cloud development. The temperature range where simulated INP_{PBAP} exhibit considerable concentrations (1 L^{-1}, < -12°C) aligns closely with the temperature range where secondary ice is expected to be active -5ºC to -20ºC (Korolev and Leisner, 2020), with peak impact around -15 ºC (Georgakaki et al., 2022). Although not contributing significant primary ice particles, INP_{PBAP} at warmer freezing temperatures may help sustain high concentrations of secondary ice, by contributing primary ice necessary for SIP. That said, SIP is most effective for situations where there are seeder-feeder cloud configurations (i.e., layered clouds or vertically developed clouds that have internal seeding; Georgakaki and Nenes, 2023) so it remains to be investigated whether the “niche” impact of INP from PBAP on SIP is climatically important.

To illustrate the various components of INP depending on atmospheric temperature, figure 3 presents the INP total number concertation column (up to 300 hPa) sampled from the model results for three different

https://doi.org/10.5194/egusphere-2024-952
Preprint. Discussion started: 19 April 2024

air temperature ranges [-40 °C to -30 °C (Fig. 3a), -30 °C to -20 °C (Fig. 3b) and -20 °C to -10 °C (Fig. 3c)]. We also present the annual mean percentage contribution from mineral dust, MPOA and PBAP for these columns. Figure 3 clearly shows that PBAP are the main INP precursor in temperatures ranging from -20°C to -10°C in both hemispheres while MPOA and mineral dust are the primary source of INP at lower temperatures. Additionally, for temperature range between -40 °C to -30 °C (Fig. 3a) and -30 °C to -20 °C (Fig. 3b) mineral dust emerges as the dominant source of INP (more than 90%) in NH while MPOA are the main source in SH (more than 75%).

The zonal distribution of INP exhibits a notable altitude-dependent variation in the contribution of INP precursors. As discussed, INP_D dominate at high altitudes, whereas INP_{PBAP} and INP_{MPOA} dominate at low altitudes. Figure 4 provides a comprehensive insight into the global contribution of distinct INP sources and establishes a correlation between the percentage contribution of each INP type and the concentration ranges of INP. The INP column burdens (m^{-2}) from surface up to 600 hPa (Fig. 4a) and up to 300 hPa (Fig. 4b) are depicted, along with the seasonal percentage contribution of the three different types of INP in the SH and NH. The INP column up to 600 hPa (Fig. 4a) reveals that mineral dust is the dominant INP precursor in the NH during boreal winter and spring (DJF, MAM), accounting for ~75% on average. During summer and autumn (JJA, SON), PBAP emerges as the primary source of INP, which strongly correlates with vegetation growth, as aforementioned. The contribution of MPOA remains minor across all seasons, accounting for almost 10%. In contrast, in the SH, the dominant source of INP is MPOA (about 83 % of the INP column up to 600 hPa), followed by dust (about 17%), while the contribution of PBAP is almost negligible (about 2.5%). However, it should be noted that in equatorial regions where the major sources of PBAP are located, ice nucleation occurs at pressures lower than 600 hPa. This explains the small contribution of PBAP up to 600hPa.

The INP column burden up to 300 hPa is depicted in Figure 4b. Mineral dust serves as the predominant INP precursor in the NH across all seasons (at least 50%), accounting for 68% of the column on annual average. INP_{PBAP} represents ~27% of the INP column, with an increased contribution during the boreal summer and fall months (~45%). The contribution of INP_{MPOA} is small, about 5%. Conversely, the major contributor to the INP population in the SH is MPOA, representing on annual average approximately 46% of the total INP column. It is followed by INP_{PBAP} at about 30%, which is maximized in the austral summer (DJF, 35%), while mineral dust plays a comparatively minor role, contributing ~24%. This is partly attributed to the low fraction of K-feldspar minerals estimated to be present in dust particles emitted from the Patagonian and the Kalahari Deserts (Journet et al., 2014; Nickovic et al., 2012). The amount of simulated INP is greater in the NH than in the SH, which is in agreement with previous studies (Vergara-Temprado et al., 2017).

Figure 5(a-c) depicts the simulated distributions of INP derived from each studied aerosol type present at 600 hPa and with the ability to freeze at -20°C in immersion mode (hereafter called INP_{-20}). These conditions of temperature and pressure are representative of MPC's glaciation and allow all species to activate and act as INP. In addition, the simulation of INP concentration at specific temperatures (e.g., -20°C) is required to compare modelled and observed INP concentrations, since the measurements of INP concentrations are determined by exposing particles to controlled temperatures within the

https://doi.org/10.5194/egusphere-2024-952
Preprint. Discussion started: 19 April 2024

instrumentation. Figure 5d shows the total INP distribution calculated accounting for all the aforementioned tracers.

The concentrations of $INP_{D\text{-}20}$ (Fig. 5a) contribute much more to mid-latitude INP concentrations in the NH than in the SH due to long-range atmospheric transport patterns from sources that favour dust present in the NH. Throughout much of the low and mid-latitudes of the NH, $INP_{D\text{-}20}$ outnumbers by far $INP_{MPOA\text{-}20}$ and $INP_{PBAP\text{-}20}$ (Fig. 5a-c). $INP_{MPOA\text{-}20}$ dominates in the oceanic regions, in particular those in the SH, and $INP_{PBAP\text{-}20}$ prevails over tropical and equatorial continental sites and up to +/- 40º latitude. However, there are oceanic regions in the South Atlantic Ocean (such as the West coast of S. Africa and the North west coast of S. America) where PBAP has the potential to form ice crystals at the outflow of the continental air (Fig. 5b) and in the middle and high troposphere (Fig. 2e), enhancing INP concentrations in marine environments.

3.2 Comparing predictions with observations

Cloud-resolved high-resolution modeling studies indicate that clouds can present sensitivity to INP perturbations that exceed one order of magnitude (Fan et al., 2017). For the simulation of INP in models to be deemed satisfactory, prediction errors must be constrained to less than an order of magnitude for the majority of observations (Cornwell et al., 2023). Figure 6 shows the comparison of INP observations with simulated INP, for each INP precursor separately and for all possible combinations. Two metrics are used to assess the ability of the model to correctly predict INP concentrations for each of the depicted cases and are reported in this Figure: i) the percentage of INP simulated values within one order of magnitude from the observed values (Pt_1) and ii) the percentage within one and half orders of magnitude ($Pt_{1.5}$). The correlation between observed and predicted INP is presented by the correlation coefficient (R).

Considering dust minerals as the sole INP precursors leads to underestimation against observations (Fig. 6a). Even if dust is the most abundant aerosol in the atmosphere, the simulated dust-derived INP cannot predict the observed INP, especially at high temperatures (>-15ºC). Mineral dust particles likely become ice-active only at low temperatures (Chatziparaschos et al., 2023; Cornwell et al., 2023). However, there are large uncertainties in this hypothesis since dust minerals may be carriers of biogenic ice-active matter (Hill et al., 2016; O'Sullivan et al., 2016), which enhances dust nucleation activity at higher temperatures. The existence of PBAP onto mineral dust and their effect on its ice nucleating activity requires dedicated studies and improved parameterizations. These findings are largely in agreement with the literature and have been thoroughly discussed in Chatziparaschos et al. (2023).

INP_{MPOA} alone significantly improves the prediction of the observed INP at high temperatures, increasing the predictability of the model to 70% (Pt_1, Fig. 6b). However, this improvement is accompanied by a decrease in correlation coefficient (R). At low (<-30ºC) and mid (-20ºC) temperatures INP_{MPOA} underestimates the observations (Fig. 6b). The discrepancy between observed INP and INP_{MPOA} estimated from the Wilson et al. (2015) relationship may suggest a deficiency in the relationship used between Chl-a concentrations and MPOA emissions (McCluskey et al., 2017). In addition, it has been previously reported by McCluskey et al. (2018) that the Wilson et al. (2015) parameterization may

https://doi.org/10.5194/egusphere-2024-952
Preprint. Discussion started: 19 April 2024

overpredict INP. Nevertheless, our findings do not support this outcome. The model results tend to slightly overpredict INP only in the temperature range around -25 °C. Wilson et al. (2015) identified a temperature-dependent relationship between total organic carbon mass and ice-nucleating entity (Vali et al., 2015) number concentrations in sea surface microlayer samples, while the McCluskey et al. (2018) parameterization has no explicit dependence on the organic carbon content of SS. The Wilson et al. (2015) parameterization was empirically derived from observations of ambient SS, proposing ice nucleation site densities (INP per square meter of aerosol) associated with SS surface area. This approach requires the quantification of SS size distributions and detailed organic composition, taking into account the SS size variability that occurred due to marine biological processes; this process is not parameterized in McCluskey et al. (2018). However, there is clear evidence of the link between marine organic matter and INP activity (McCluskey et al., 2017, 2018; Wilson et al., 2015) and both the amount and the composition of organic components included in the SS are a strong function of particles size (Wang et al., 2017; O'Dowd et al., 2004). Therefore, our model, which calculates INP using the Wilson et al. (2015) parameterization and accounts for the MPOA mass dependence on the presence of Chl-a (Vignati et al., 2010) and for the MPOA ageing process (section 2.2), may provide a more realistic approach. These findings indicate that the representation of SS significantly influences INP, emphasizing the need for future studies to accurately quantify sea spray size distributions and detailed organic composition.

Figure 6c shows the comparison between simulated INP_{PBAP} and observed INP. INP_{PBAP} overestimate the observed INP across temperature ranges warmer than -30°C, followed by a subsequent underestimation beyond this temperature. The model's predictability increases (Pt_1 = 61%) compared to INP_D (Pt_1 = 51%) but decreases compared to INP_{MPOA} (Pt_1 ~70%). This overall overestimation could be attributed to uncertainties in parameterizations for the ice nuclei activity of PBAP or to our model performance. It has been proved from laboratory studies that the ice nuclei activity of bacterial and fungal spores can vary substantially across different species (Pummer et al., 2012; Murray et al., 2012). The species composition of airborne fungal and bacterial communities exhibits considerable geographic variability (Dietzel et al., 2019). Thus, it is reasonable to expect that the ice efficiency of airborne PBAP may strongly differ geographically. The INP parameterizations we have used were developed based on a small number of samples from the mid-latitudinal ponderosa pine forest ecosystem (Tobo et al., 2013) and may not be representative of the global simulation of INP_{PBAP}. On the other hand, our model is able to simulate the mean number and mass concentrations of PBAP within the correct order of magnitude, and seasonal cycles and regional-scale geographic distributions that correlate with observed patterns; however, it slightly overestimates the BCT and FNG burden, as reported by Myriokefalitakis et al. (2017). This could impact the simulated INP_{PBAP}, contributing to this observed overestimation. Overall, among the three different types of INP when considered individually the highest correlation is found for INP_D.

The model's agreement with the INP observations is moderate, with a correlation coefficient of 0.87 and about 59% (Pt_1) predictability when considering all INP types (Fig. 6f). Considering only mineral dust and MPOA (Fig. 6d) improves the predictive ability of the model (about 73%, Pt_1) and has the highest correlation coefficient 0.88 (Fig. 6c). The inclusion of MPOA improves the model's comparison between -6°C and -25°C where MPOA exhibits high ice activity. Model results are more consistent with observations, with the model reproducing about 73% of observations within an order of magnitude and

https://doi.org/10.5194/egusphere-2024-952
Preprint. Discussion started: 19 April 2024

about 87% within one and a half orders of magnitude, as illustrated in Figure 6d. These findings suggest that for climate prediction, with the current knowledge of ice nuclei properties of dust, PBAP and MPOA, consideration of mineral dust and MPOA as the main contributor to INP globally could be sufficient. Dust particles typically have ice nucleating activities up to two to three orders of magnitude greater than marine particles at the same temperature (Cornwell et al., 2023; McCluskey et al., 2018); however the INP_{MPOA} concentration depends on the location and the altitude of the measurements. Marine particles are an important source of INP at locations distant from land. Including INP_{PBAP} in the simulations in addition to INP_D and INP_{MPOA} leads to an overestimation of measurements and reduces the accuracy of the model's predictions (Fig. 6f). In no case should this diminish the role of INP derived from PBAP, especially in regions where PBAP is more abundant or ecosystems are diverse, such as the Amazon, affecting INP concentrations locally (Prenni et al., 2009). Most of the INP at warmer temperatures than -16°C are bioaerosols, suggesting that without improved representations of the sources and ice-nucleating activities of biological INP, models will struggle to simulate total INP concentrations at warmer temperatures and the resulting MPC.

Other sources of model bias may be attributed to atmospheric processes, such as the ageing of aerosols that results in the degradation of ice-nucleation activity. For instance, ageing with sulfuric acid can either greatly reduce the immersion mode ice-nucleation activity or have little effect (Kumar et al., 2019a, b; Jahl et al., 2021). Although there are conflicting findings and limited understanding regarding how to parameterize the ice-nucleation activity of aged particles, potential ageing effects directly on INP are not considered in our study. The effects of atmospheric ageing on ice-nucleating activity are probably a minor source of error in this study, in comparison to the introduced bias from the employed INP parameterizations and model performance.

In summary, the comparison of model results with observations reveals that dust particles are a minor INP source at warm temperatures, but increase in importance at colder temperatures. INP at temperatures in the vicinity of zero are typically related to INP from biogenic sources. These findings are consistent with previous observational studies showing that biological INP make up a greater fraction of continental INP at warm temperatures (Mason et al., 2015; Gong et al., 2022). The model achieves its highest predictability and correlation against observed INP across all temperature ranges when both INP_D and INP_{MPOA} are included.

4 Conclusions

In this study, we performed global model simulations of mineral dust, primary marine organic aerosols, and terrestrial bioaerosol (bacterial and fungal spores) and investigated their contribution to atmospheric ice nucleation using laboratory-derived parameterizations based on the singular description approach. At relatively warm temperatures (warmer than −20 °C), the majority of INP are typically of biological origin, while at lower temperatures and higher altitudes, INP from mineral dust dominates globally. INP from dust contributes more to total INP in the mid-latitudes in the NH than in the SH due to the location of the dust sources and the long-range atmospheric transport patterns. INP from terrestrial bioaerosol peaks in the low and mid-troposphere and could be important in reproducing/representing atmospheric INP populations at warm temperatures. Concentrations of INP from terrestrial bioaerosol vary depending

https://doi.org/10.5194/egusphere-2024-952
Preprint. Discussion started: 19 April 2024

on the season and regional weather patterns. INP from terrestrial bioaerosol has the potential to form ice crystals in the NH subtropics at the outflow of the continental air. INP from marine bioaerosol are primarily found over oceans and coastal areas and dominate between 40°-90°S (Southern Ocean), with high concentrations in regions of high sea spray and phytoplankton activity.

The model achieves its highest predictability against observed INP across all temperature ranges when both INP_D and INP_{MPOA} are included. Further inclusion of PBAP in our model leads to an overestimation of the measurements. Our study suggests that INP_D and INP_{MPOA} could sufficiently predict observed INP concentrations globally. However, bioaerosols are an important source of warm-temperature INP, affecting mainly at low altitudes.

Therefore, we propose a scheme designed to predict INP global distribution based on the most influential precursors for in-cloud ice initiation, namely mineral dust, MPOA and PBAP. The current model biases could be attributed to the uncertainties in the parameterizations for the ice-nucleating activity of each particle type, simplified source functions for particle emissions, and description of aerosol transport. Uncertainties exist, particularly with regard to the impact of atmospheric mixing and processing of different INP species on INP properties. For instance, dust minerals could be carriers of biogenic ice-active macromolecules and bioaerosol or be coated by sulphate and/or nitrate or other pollutants during the atmospheric ageing of dust (Iwata and Matsuki, 2018). These processes are at present neglected or heavily parameterized in our model and could lead to the enhancement or reduction of INP ice-activation properties. For example, ammonium salts can cause suspended particles of feldspars and quartz to nucleate ice at substantially higher temperatures than they do in pure water (Whale et al., 2018). Conversely, sulfate acids can dramatically depress freezing for the aforementioned nucleators. Future studies should investigate the impact of atmospheric mixing and ageing on INP concentrations and constrain them by measurements over receptor areas downwind of source regions. Tackling these research priorities is essential for developing a more comprehensive understanding of the atmospheric variability of INP and their impacts in different cloud regimes.

Acknowledgements. This work has been supported by the European Union Horizon 2020 project FORCeS under grant agreement No 821205. The early stages of this work have been supported by the project "PANhellenic infrastructure for Atmospheric Composition and climatE change" (PANACEA; MIS 5021516), which is implemented under the Action "Reinforcement of the Research and Innovation Infrastructure", funded by the Operational Programme "Competitiveness, Entrepreneurship and Innovation" (NSRF 2014-2020) and co-financed by Greece and the European Union (European Regional Development Fund). ND, MK and MV acknowledge support from the Deutsche Forschungsgemeinschaft (DFG) under Germany´s Excellence Strategy (University Allowance, EXC 2077, University of Bremen). CPG-P, MC-S, MGA, and MC acknowledge support from the European Research Council under the European Union's Horizon 2020 research and innovation programme (grant n. 773051; FRAGMENT) and from the AXA Research Fund. MC-S has received funding from the European Union's Horizon 2020 research and innovation programme, under the Marie Skłodowska-Curie grant agreements, reference 754433 from the call H2020-MSCA-COFUND-2016. AN acknowledges support from project Pyro-TRACH (ERC-2016-COG) funded from H2020-EU.1.1. - Excellent Science - European Research Council (ERC), project ID 726165.

Author contributions. MK and MC conceived the study. MC modified the model to account for INP and performed the simulations, visualized and analyzed data, and wrote the initial version of the paper. MK supervised the work with feedback from AN and CPG-P and MK and CPG-P re-edited the paper.

https://doi.org/10.5194/egusphere-2024-952
Preprint. Discussion started: 19 April 2024

All authors provided scientific feedback contributed to the review and guidance, commented and provided revisions in subsequent versions editing of the paper before submission.

Competing interests. Some authors are members of the editorial board of journal Atmospheric Chemistry and Physics.

References

Ansmann, A., Tesche, M., Althausen, D., Müller, D., Seifert, P., Freudenthaler, V., Heese, B., Wiegner, M., Pisani, G., Knippertz, P., and Dubovik, O.: Influence of Saharan dust on cloud glaciation in southern Morocco during the Saharan Mineral Dust Experiment, J. Geophys. Res., 113, D04210, https://doi.org/10.1029/2007JD008785, 2008.

Atkinson, J. D., Murray, B. J., Woodhouse, M. T., Whale, T. F., Baustian, K. J., Carslaw, K. S., Dobbie, S., O'Sullivan, D., and Malkin, T. L.: The importance of feldspar for ice nucleation by mineral dust in mixed-phase clouds., Nature, 498, 355–8, https://doi.org/10.1038/nature12278, 2013.

Augustin-Bauditz, S., Wex, H., Kanter, S., Ebert, M., Niedermeier, D., Stolz, F., Prager, A., and Stratmann, F.: The immersion mode ice nucleation behavior of mineral dusts: A comparison of different pure and surface modified dusts, Geophys. Res. Lett., 41, 7375–7382, https://doi.org/10.1002/2014GL061317, 2014.

Augustin-Bauditz, S., Wex, H., Denjean, C., Hartmann, S., Schneider, J., Schmidt, S., Ebert, M., and Stratmann, F.: Laboratory-generated mixtures of mineral dust particles with biological substances: characterization of the particle mixing state and immersion freezing behavior, Atmos. Chem. Phys., 16, 5531–5543, https://doi.org/10.5194/acp-16-5531-2016, 2016.

Billault-Roux, A.-C., Georgakaki, P., Gehring, J., Jaffeux, L., Schwarzenboeck, A., Coutris, P., Nenes, A., and Berne, A.: Distinct secondary ice production processes observed in radar Doppler spectra: insights from a case study, Atmos. Chem. Phys., 23, 10207–10234, https://doi.org/10.5194/acp-23-10207-2023, 2023.

Bodas-Salcedo, A., Hill, P. G., Furtado, K., Williams, K. D., Field, P. R., Manners, J. C., Hyder, P., and Kato, S.: Large Contribution of Supercooled Liquid Clouds to the Solar Radiation Budget of the Southern Ocean, J. Clim., 29, 4213–4228, https://doi.org/10.1175/JCLI-D-15-0564.1, 2016.

Bones, D. L., Henricksen, D. K., Mang, S. A., Gonsior, M., Bateman, A. P., Nguyen, T. B., Cooper, W. J., and Nizkorodov, S. A.: Appearance of strong absorbers and fluorophores in limonene-O 3 secondary organic aerosol due to NH 4 + -mediated chemical aging over long time scales, J. Geophys. Res. Atmos., 115, 1–14, https://doi.org/10.1029/2009JD012864, 2010.

Boose, Y., Welti, A., Atkinson, J., Ramelli, F., Danielczok, A., Bingemer, H. G., Plötze, M., Sierau, B., Kanji, Z. A., and Lohmann, U.: Heterogeneous ice nucleation on dust particles sourced from nine deserts worldwide – Part 1: Immersion freezing, Atmos. Chem. Phys., 16, 15075–15095, https://doi.org/10.5194/acp-16-15075-2016, 2016.

Boose, Y., Baloh, P., Plötze, M., Ofner, J., Grothe, H., Sierau, B., Lohmann, U., and Kanji, Z. A.: Heterogeneous ice nucleation on dust particles sourced from nine deserts worldwide - Part 2: Deposition nucleation and condensation freezing, Atmos. Chem. Phys., 19, 1059–1076, https://doi.org/10.5194/acp-19-1059-2019, 2019.

Borys, R. D., Lowenthal, D. H., Cohn, S. A., and Brown, W. O. J.: Mountaintop and radar measurements of anthropogenic aerosol effects on snow growth and snowfall rate, Geophys. Res. Lett., 30, https://doi.org/https://doi.org/10.1029/2002GL016855, 2003.

Burrows, S. M., Butler, T., Jöckel, P., Tost, H., Kerkweg, a., Pöschl, U., and Lawrence, M. G.: Bacteria in the global atmosphere – Part 2: Modelling of emissions and transport between different ecosystems, Atmos. Chem. Phys. Discuss., 9, 10829–10881, https://doi.org/10.5194/acpd-9-10829-2009, 2009.

Burrows, S. M., Hoose, C., Pöschl, U., and Lawrence, M. G.: Ice nuclei in marine air: Biogenic particles or dust?,

https://doi.org/10.5194/egusphere-2024-952
Preprint. Discussion started: 19 April 2024

Atmos. Chem. Phys., 13, 245–267, https://doi.org/10.5194/acp-13-245-2013, 2013.

Burrows, S. M., McCluskey, C. S., Cornwell, G., Steinke, I., Zhang, K., Zhao, B., Zawadowicz, M., Raman, A., Kulkarni, G., China, S., Zelenyuk, A., and DeMott, P. J.: Ice-Nucleating Particles That Impact Clouds and Climate: Observational and Modeling Research Needs, https://doi.org/10.1029/2021RG000745, 16 June 2022.

Chatziparaschos, M., Daskalakis, N., Myriokefalitakis, S., Kalivitis, N., Nenes, A., Gonçalves Ageitos, M., Costa-Surós, M., Pérez Garc\'\ia-Pando, C., Zanoli, M., Vrekoussis, M., and Kanakidou, M.: Role of K-feldspar and quartz in global ice nucleation by mineral dust in mixed-phase clouds, Atmos. Chem. Phys., 23, 1785–1801, https://doi.org/10.5194/acp-23-1785-2023, 2023.

Chen, J., Wu, Z., Chen, J., Reicher, N., Fang, X., Rudich, Y., and Hu, M.: Size-resolved atmospheric ice-nucleating particles during East Asian dust events, Atmos. Chem. Phys., 21, 3491–3506, https://doi.org/10.5194/acp-21-3491-2021, 2021.

Choi, Y.-S., Ho, C.-H., Park, C.-E., Storelvmo, T., and Tan, I.: Influence of cloud phase composition on climate feedbacks, J. Geophys. Res. Atmos., 119, 3687–3700, https://doi.org/10.1002/2013JD020582, 2014.

Chubb, T. H., Jensen, J. B., Siems, S. T., and Manton, M. J.: In situ observations of supercooled liquid clouds over the Southern Ocean during the HIAPER Pole-to-Pole Observation campaigns, Geophys. Res. Lett., 40, 5280–5285, https://doi.org/10.1002/grl.50986, 2013.

Claquin, T., Schulz, M., and Balkanski, Y. J.: Modeling the mineralogy of atmospheric dust sources, J. Geophys. Res. Atmos., 104, 22243–22256, https://doi.org/10.1029/1999JD900416, 1999.

Cooke, W. F., Liousse, C., Cachier, H., and Feichter, J.: Construction of a 1° × 1° fossil fuel emission data set for carbonaceous aerosol and implementation and radiative impact in the ECHAM4 model, J. Geophys. Res. Atmos., 104, 22137–22162, https://doi.org/10.1029/1999JD900187, 1999.

Cornwell, G., McCluskey, C., Hill, T. C., Levin, E., Rothfuss, N., Tai, S.-L., Petters, M. D., DeMott, P. J., Kreidenweis, S., Prather, K., and Burrows, S. M.: Dataset for "Bioaerosols are the dominant source of warm-temperature immersion-mode INPs and drive uncertainties in INP predictability, https://doi.org/10.25584/1890223, 2022.

Cornwell, G. C., McCluskey, C. S., Hill, T. C. J., Levin, E. T., Rothfuss, N. E., Tai, S.-L., Petters, M. D., DeMott, P. J., Kreidenweis, S., Prather, K. A., and Burrows, S. M.: Bioaerosols are the dominant source of warm-temperature immersion-mode INPs and drive uncertainties in INP predictability, Sci. Adv., 9, eadg3715, https://doi.org/10.1126/sciadv.adg3715, 2023.

Creamean, J. M., Barry, K., Hill, T. C. J., Hume, C., DeMott, P. J., Shupe, M. D., Dahlke, S., Willmes, S., Schmale, J., Beck, I., Hoppe, C. J. M., Fong, A., Chamberlain, E., Bowman, J., Scharien, R., and Persson, O.: Annual cycle observations of aerosols capable of ice formation in central Arctic clouds, Nat. Commun., 13, 3537, https://doi.org/10.1038/s41467-022-31182-x, 2022.

Cziczo, D. J., Froyd, K. D., Hoose, C., Jensen, E. J., Diao, M., Zondlo, M. A., Smith, J. B., Twohy, C. H., and Murphy, D. M.: Clarifying the Dominant Sources and Mechanisms of Cirrus Cloud Formation, Science (80-.)., 340, 1320–1324, https://doi.org/10.1126/science.1234145, 2013.

D'Alessandro, J. J., Diao, M., Wu, C., Liu, X., Jensen, J. B., and Stephens, B. B.: Cloud Phase and Relative Humidity Distributions over the Southern Ocean in Austral Summer Based on In Situ Observations and CAM5 Simulations, J. Clim., 32, 2781–2805, https://doi.org/10.1175/JCLI-D-18-0232.1, 2019.

Dee, D. P., Uppala, S. M., Simmons, A. J., Berrisford, P., Poli, P., Kobayashi, S., Andrae, U., Balmaseda, M. A., Balsamo, G., Bauer, P., Bechtold, P., Beljaars, A. C. M., van de Berg, L., Bidlot, J., Bormann, N., Delsol, C., Dragani, R., Fuentes, M., Geer, A. J., Haimberger, L., Healy, S. B., Hersbach, H., Hólm, E. V., Isaksen, L., Kållberg, P., Köhler, M., Matricardi, M., Mcnally, A. P., Monge-Sanz, B. M., Morcrette, J. J., Park, B. K., Peubey, C., de Rosnay, P., Tavolato, C., Thépaut, J. N., and Vitart, F.: The ERA-Interim reanalysis: Configuration and performance of the data assimilation system, Q. J. R. Meteorol. Soc., 137, 553–597, https://doi.org/10.1002/qj.828, 2011.

DeMott, P. J. and Prenni, A. J.: New Directions: Need for defining the numbers and sources of biological aerosols

https://doi.org/10.5194/egusphere-2024-952
Preprint. Discussion started: 19 April 2024

acting as ice nuclei, Atmos. Environ., 44, 1944–1945, https://doi.org/10.1016/j.atmosenv.2010.02.032, 2010.

DeMott, P. J., Prenni, A. J., Liu, X., Kreidenweis, S. M., Petters, M. D., Twohy, C. H., Richardson, M. S., Eidhammer, T., and Rogers, D. C.: Predicting global atmospheric ice nuclei distributions and their impacts on climate., Proc. Natl. Acad. Sci., 107, 11217–22, https://doi.org/10.1073/pnas.0910818107, 2010.

Dietzel, K., Valle, D., Fierer, N., U'Ren, J. M., and Barberán, A.: Geographical Distribution of Fungal Plant Pathogens in Dust Across the United States, Front. Ecol. Evol., 7, 1–8, https://doi.org/10.3389/fevo.2019.00304, 2019.

Facchini, M. C., Decesari, S., Rinaldi, M., Carbone, C., Finessi, E., Mircea, M., Fuzzi, S., Moretti, F., Tagliavini, E., Ceburnis, D., and O'Dowd, C. D.: Important source of marine secondary organic aerosol from biogenic amines., Environ. Sci. Technol., 42, 9116–21, https://doi.org/10.1021/es8018385, 2008.

Fan, J., Ruby Leung, L., Rosenfeld, D., and Demott, P. J.: Effects of cloud condensation nuclei and ice nucleating particles on precipitation processes and supercooled liquid in mixed-phase orographic clouds, Atmos. Chem. Phys., 17, 1017–1035, https://doi.org/10.5194/acp-17-1017-2017, 2017.

Frey, W. R. and Kay, J. E.: The influence of extratropical cloud phase and amount feedbacks on climate sensitivity, Clim. Dyn., 50, 3097–3116, https://doi.org/10.1007/s00382-017-3796-5, 2018.

Georgakaki, P. and Nenes, A.: RaFSIP: Parameterizing ice multiplication in models using a machine learning approach, https://doi.org/10.22541/essoar.170365383.34520011/v1, 2023.

Georgakaki, P., Sotiropoulou, G., Vignon, É., Billault-Roux, A.-C., Berne, A., and Nenes, A.: Secondary ice production processes in wintertime alpine mixed-phase clouds, Atmos. Chem. Phys., 22, 1965–1988, https://doi.org/10.5194/acp-22-1965-2022, 2022.

Ginoux, P., Prospero, J. M., Torres, O., and Chin, M.: Long-term simulation of global dust distribution with the GOCART model: Correlation with North Atlantic Oscillation, Environ. Model. Softw., 19, 113–128, https://doi.org/10.1016/S1364-8152(03)00114-2, 2004.

Glaccum, R. A. and Prospero, J. M.: Saharan aerosols over the tropical North Atlantic — Mineralogy, Mar. Geol., 37, 295–321, https://doi.org/10.1016/0025-3227(80)90107-3, 1980.

Gong, S. L.: A parameterization of sea-salt aerosol source function for sub- and super-micron particles, Global Biogeochem. Cycles, https://doi.org/10.1029/2003GB002079, 2003.

Gong, X., Radenz, M., Wex, H., Seifert, P., Ataei, F., Henning, S., Baars, H., Barja, B., Ansmann, A., and Stratmann, F.: Significant continental source of ice-nucleating particles at the tip of Chile's southernmost Patagonia region, Atmos. Chem. Phys., 22, 10505–10525, https://doi.org/10.5194/acp-22-10505-2022, 2022.

Hande, L. B. and Hoose, C.: Partitioning the primary ice formation modes in large eddy simulations of mixed-phase clouds, Atmos. Chem. Phys., 17, 14105–14118, https://doi.org/10.5194/acp-17-14105-2017, 2017.

Harrison, A. D., Lever, K., Sanchez-Marroquin, A., Holden, M. A., Whale, T. F., Tarn, M. D., McQuaid, J. B., and Murray, B. J.: The ice-nucleating ability of quartz immersed in water and its atmospheric importance compared to K-feldspar, Atmos. Chem. Phys. Discuss., 1–23, https://doi.org/10.5194/acp-2019-288, 2019.

Heald, C. L. and Spracklen, D. V: Atmospheric budget of primary biological aerosol particles from fungal spores, Geophys. Res. Lett., 36, L09806, https://doi.org/10.1029/2009GL037493, 2009.

Hill, T. C. J., Demott, P. J., Tobo, Y., Fröhlich-Nowoisky, J., Moffett, B. F., Franc, G. D., and Kreidenweis, S. M.: Sources of organic ice nucleating particles in soils, Atmos. Chem. Phys., 16, 7195–7211, https://doi.org/10.5194/acp-16-7195-2016, 2016.

Holden, M. A., Whale, T. F., Tarn, M. D., O'Sullivan, D., Walshaw, R. D., Murray, B. J., Meldrum, F. C., and Christenson, H. K.: High-speed imaging of ice nucleation in water proves the existence of active sites, Sci. Adv., 5, eaav4316, https://doi.org/10.1126/sciadv.aav4316, 2019.

Hoose, C. and Möhler, O.: Heterogeneous ice nucleation on atmospheric aerosols: A review of results from laboratory experiments, 9817-9854 pp., https://doi.org/10.5194/acp-12-9817-2012, 2012.

Hoose, C., Lohmann, U., Erdin, R., and Tegen, I.: The global influence of dust mineralogical composition on heterogeneous ice nucleation in mixed-phase clouds, Environ. Res. Lett., 3, 025003,

https://doi.org/10.5194/egusphere-2024-952
Preprint. Discussion started: 19 April 2024

https://doi.org/10.1088/1748-9326/3/2/025003, 2008.

Hoose, C., Kristjánsson, J. E., and Burrows, S. M.: How important is biological ice nucleation in clouds on a global scale?, Environ. Res. Lett., 5, 024009, https://doi.org/10.1088/1748-9326/5/2/024009, 2010.

Huang, S., Hu, W., Chen, J., Wu, Z., Zhang, D., and Fu, P.: Overview of biological ice nucleating particles in the atmosphere, Environ. Int., 146, 106197, https://doi.org/10.1016/j.envint.2020.106197, 2021.

Huang, W. T. K., Ickes, L., Tegen, I., Rinaldi, M., Ceburnis, D., and Lohmann, U.: Global relevance of marine organic aerosol as ice nucleating particles, Atmos. Chem. Phys., 18, 11423–11445, https://doi.org/10.5194/acp-18-11423-2018, 2018.

Huffman, J. A., Prenni, A. J., DeMott, P. J., Pöhlker, C., Mason, R. H., Robinson, N. H., Fröhlich-Nowoisky, J., Tobo, Y., Després, V. R., Garcia, E., Gochis, D. J., Harris, E., Müller-Germann, I., Ruzene, C., Schmer, B., Sinha, B., Day, D. A., Andreae, M. O., Jimenez, J. L., Gallagher, M., Kreidenweis, S. M., Bertram, A. K., and Pöschl, U.: High concentrations of biological aerosol particles and ice nuclei during and after rain, Atmos. Chem. Phys., 13, 6151–6164, https://doi.org/10.5194/acp-13-6151-2013, 2013.

Hummel, M., Hoose, C., Gallagher, M., Healy, D. A., Huffman, J. A., O'Connor, D., Pöschl, U., Pöhlker, C., Robinson, N. H., Schnaiter, M., Sodeau, J. R., Stengel, M., Toprak, E., and Vogel, H.: Regional-scale simulations of fungal spore aerosols using an emission parameterization adapted to local measurements of fluorescent biological aerosol particles, Atmos. Chem. Phys., 15, 6127–6146, https://doi.org/10.5194/acp-15-6127-2015, 2015.

Jahl, L. G., Brubaker, T. A., Polen, M. J., Jahn, L. G., Cain, K. P., Bowers, B. B., Fahy, W. D., Graves, S., and Sullivan, R. C.: Atmospheric aging enhances the ice nucleation ability of biomass-burning aerosol, Sci. Adv., 7, 1–10, https://doi.org/10.1126/sciadv.abd3440, 2021.

Jeuken, M., Van Wijk, R., Peleman, J., and Lindhout, P.: An integrated interspecific AFLP map of lettuce (Lactuca) based on two L. sativa × L. saligna F2 populations, Theor. Appl. Genet., 103, 638–647, https://doi.org/10.1007/s001220100657, 2001.

Journet, E., Balkanski, Y., and Harrison, S. P.: A new data set of soil mineralogy for dust-cycle modeling, Atmos. Chem. Phys., 14, 3801–3816, https://doi.org/10.5194/acp-14-3801-2014, 2014.

Kanakidou, M., Duce, R. A., Prospero, J. M., Baker, A. R., Benitez-Nelson, C., Dentener, F. J., Hunter, K. A., Liss, P. S., Mahowald, N., Okin, G. S., Sarin, M., Tsigaridis, K., Uematsu, M., Zamora, L. M., and Zhu, T.: Atmospheric fluxes of organic N and P to the global ocean, Global Biogeochem. Cycles, 26, 1–12, https://doi.org/10.1029/2011GB004277, 2012.

Kanakidou, M., Myriokefalitakis, S., and Tsagkaraki, M.: Atmospheric inputs of nutrients to the Mediterranean Sea, Deep. Res. Part II Top. Stud. Oceanogr., 171, https://doi.org/10.1016/j.dsr2.2019.06.014, 2020.

Kanji, Z. A., Ladino, L. A., Wex, H., Boose, Y., Burkert-Kohn, M., Cziczo, D. J., and Krämer, M.: Overview of Ice Nucleating Particles, Meteorol. Monogr., 58, 1.1-1.33, https://doi.org/10.1175/AMSMONOGRAPHS-D-16-0006.1, 2017.

Kluska, K., Piotrowicz, K., and Kasprzyk, I.: The impact of rainfall on the diurnal patterns of atmospheric pollen concentrations, Agric. For. Meteorol., 291, 108042, https://doi.org/10.1016/j.agrformet.2020.108042, 2020.

Kok, J. F.: A scaling theory for the size distribution of emitted dust aerosols suggests climate models underestimate the size of the global dust cycle, Proc. Natl. Acad. Sci. U. S. A., 108, 1016–1021, https://doi.org/10.1073/pnas.1014798108, 2011.

Korolev, A.: Limitations of the Wegener–Bergeron–Findeisen Mechanism in the Evolution of Mixed-Phase Clouds, J. Atmos. Sci., 64, 3372–3375, https://doi.org/10.1175/JAS4035.1, 2007.

Korolev, A. and Leisner, T.: Review of experimental studies of secondary ice production, Atmos. Chem. Phys., 20, 11767–11797, https://doi.org/10.5194/acp-20-11767-2020, 2020.

Korolev, A. and Milbrandt, J.: How Are Mixed-Phase Clouds Mixed?, Geophys. Res. Lett., 49, 1–7, https://doi.org/10.1029/2022GL099578, 2022.

Kumar, A., Marcolli, C., and Peter, T.: Ice nucleation activity of silicates and aluminosilicates in pure water and

https://doi.org/10.5194/egusphere-2024-952
Preprint. Discussion started: 19 April 2024

aqueous solutions. Part 2 – Quartz and amorphous silica, Atmos. Chem. Phys. Discuss., 1–35, https://doi.org/10.5194/acp-2018-1020, 2019a.

Kumar, A., Marcolli, C., and Peter, T.: Ice nucleation activity of silicates and aluminosilicates in pure water and aqueous solutions – Part 3: Aluminosilicates, Atmos. Chem. Phys., 19, 6059–6084, https://doi.org/10.5194/acp-19-6059-2019, 2019b.

Kumar, A., Klumpp, K., Barak, C., Rytwo, G., Plötze, M., Peter, T., and Marcolli, C.: Ice nucleation by smectites: The role of the edges, Atmos. Chem. Phys., 23, 4881–4902, https://doi.org/10.5194/acp-23-4881-2023, 2023.

Lee, H. J. (Julie), Laskin, A., Laskin, J., and Nizkorodov, S. A.: Excitation–Emission Spectra and Fluorescence Quantum Yields for Fresh and Aged Biogenic Secondary Organic Aerosols, Environ. Sci. Technol., 47, 5763–5770, https://doi.org/10.1021/es400644c, 2013.

Liu, D., Wang, Z., Liu, Z., Winker, D., and Trepte, C.: A height resolved global view of dust aerosols from the first year CALIPSO lidar measurements, J. Geophys. Res. Atmos., 113, 1–15, https://doi.org/10.1029/2007JD009776, 2008.

Liu, X., Shi, X., Zhang, K., Jensen, E. J., Gettelman, A., Barahona, D., Nenes, A., and Lawson, P.: Sensitivity studies of dust ice nuclei effect on cirrus clouds with the Community Atmosphere Model CAM5, Atmos. Chem. Phys., 12, 12061–12079, https://doi.org/10.5194/acp-12-12061-2012, 2012.

Losey, D. J., Sihvonen, S. K., Veghte, D. P., Chong, E., and Freedman, M. A.: Acidic processing of fly ash: chemical characterization, morphology, and immersion freezing, Environ. Sci. Process. Impacts, 20, 1581–1592, https://doi.org/10.1039/c8em00319j, 2018.

Louis, J.-F.: A parametric model of vertical eddy fluxes in the atmosphere, Boundary-Layer Meteorol., 17, 187–202, https://doi.org/10.1007/BF00117978, 1979.

Mason, R. H., Si, M., Li, J., Chou, C., Dickie, R., Toom-Sauntry, D., Pöhlker, C., Yakobi-Hancock, J. D., Ladino, L. A., Jones, K., Leaitch, W. R., Schiller, C. L., Abbatt, J. P. D., Huffman, J. A., and Bertram, A. K.: Ice nucleating particles at a coastal marine boundary layer site: Correlations with aerosol type and meteorological conditions, Atmos. Chem. Phys., 15, 12547–12566, https://doi.org/10.5194/acp-15-12547-2015, 2015.

McCluskey, C. S., Hill, T. C. J., Malfatti, F., Sultana, C. M., Lee, C., Santander, M. V, Beall, C. M., Moore, K. A., Cornwell, G. C., Collins, D. B., Prather, K. A., Jayarathne, T., Stone, E. A., Azam, F., Kreidenweis, S. M., and DeMott, P. J.: A Dynamic Link between Ice Nucleating Particles Released in Nascent Sea Spray Aerosol and Oceanic Biological Activity during Two Mesocosm Experiments, J. Atmos. Sci., 74, 151–166, https://doi.org/10.1175/JAS-D-16-0087.1, 2017.

McCluskey, C. S., Ovadnevaite, J., Rinaldi, M., Atkinson, J., Belosi, F., Ceburnis, D., Marullo, S., Hill, T. C. J., Lohmann, U., Kanji, Z. A., O'Dowd, C., Kreidenweis, S. M., and DeMott, P. J.: Marine and Terrestrial Organic Ice-Nucleating Particles in Pristine Marine to Continentally Influenced Northeast Atlantic Air Masses, J. Geophys. Res. Atmos., 123, 6196–6212, https://doi.org/10.1029/2017JD028033, 2018.

Mitts, B. A., Wang, X., Lucero, D. D., Beall, C. M., Deane, G. B., DeMott, P. J., and Prather, K. A.: Importance of Supermicron Ice Nucleating Particles in Nascent Sea Spray, Geophys. Res. Lett., 48, e2020GL089633, https://doi.org/https://doi.org/10.1029/2020GL089633, 2021.

Morrison, D., Crawford, I., Marsden, N., Flynn, M., Read, K., Neves, L., Foot, V., Kaye, P., Stanley, W., Coe, H., Topping, D., and Gallagher, M.: Quantifying bioaerosol concentrations in dust clouds through online UV-LIF and mass spectrometry measurements at the Cape Verde Atmospheric Observatory, Atmos. Chem. Phys., 20, 14473–14490, https://doi.org/10.5194/acp-20-14473-2020, 2020.

Murray, B. J., O'Sullivan, D., Atkinson, J. D., and Webb, M. E.: Ice nucleation by particles immersed in supercooled cloud droplets, Chem. Soc. Rev., 41, 6519, https://doi.org/10.1039/c2cs35200a, 2012.

Murray, B. J., Carslaw, K. S., and Field, P. R.: Opinion: Cloud-phase climate feedback and the importance of ice-nucleating particles, Atmos. Chem. Phys., 21, 665–679, https://doi.org/10.5194/acp-21-665-2021, 2021.

Myriokefalitakis, S., Vignati, E., Tsigaridis, K., Papadimas, C., Sciare, J., Mihalopoulos, N., Facchini, M. C., Rinaldi, M., Dentener, F. J., Ceburnis, D., Hatzianastasiou, N., O'Dowd, C. D., van Weele, M., and Kanakidou,

https://doi.org/10.5194/egusphere-2024-952
Preprint. Discussion started: 19 April 2024

M.: Global Modeling of the Oceanic Source of Organic Aerosols, Adv. Meteorol., 2010, 1–16, https://doi.org/10.1155/2010/939171, 2010.

Myriokefalitakis, S., Daskalakis, N., Mihalopoulos, N., Baker, A. R., Nenes, A., and Kanakidou, M.: Changes in dissolved iron deposition to the oceans driven by human activity: a 3-D global modelling study, Biogeosciences, 12, 3973–3992, https://doi.org/10.5194/bg-12-3973-2015, 2015.

Myriokefalitakis, S., Nenes, A., Baker, A. R., Mihalopoulos, N., and Kanakidou, M.: Bioavailable atmospheric phosphorous supply to the global ocean: a 3-D global modelling study, Biogeosciences Discuss., 0, 1–28, https://doi.org/10.5194/bg-2016-215, 2016.

Myriokefalitakis, S., Fanourgakis, G., and Kanakidou, M.: The Contribution of Bioaerosols to the Organic Carbon Budget of the Atmosphere, in: Perspectives on Atmospheric Sciences, edited by: Karacostas, T., Bais, A., and Nastos, P. T., Springer International Publishing, Cham, 845–851, https://doi.org/10.1007/978-3-319-35095-0_121, 2017.

Naud, C. M., Booth, J. F., and Genio, A. D. Del: Evaluation of ERA-Interim and MERRA Cloudiness in the Southern Ocean, J. Clim., 27, 2109–2124, https://doi.org/10.1175/JCLI-D-13-00432.1, 2014.

Negron, A., DeLeon-Rodriguez, N., Waters, S. M., Ziemba, L. D., Anderson, B., Bergin, M., Konstantinidis, K. T., and Nenes, A.: Using flow cytometry and light-induced fluorescence to characterize the variability and characteristics of bioaerosols in springtime in Metro Atlanta, Georgia, Atmos. Chem. Phys., 20, 1817–1838, https://doi.org/10.5194/acp-20-1817-2020, 2020.

Nickovic, S., Vukovic, A., Vujadinovic, M., Djurdjevic, V., and Pejanovic, G.: Technical Note: High-resolution mineralogical database of dust-productive soils for atmospheric dust modeling, Atmos. Chem. Phys., 12, 845–855, https://doi.org/10.5194/acp-12-845-2012, 2012.

Van Noije, T. P. C., Le Sager, P., Segers, A. J., Van Velthoven, P. F. J., Krol, M. C., Hazeleger, W., Williams, A. G., and Chambers, S. D.: Simulation of tropospheric chemistry and aerosols with the climate model EC-Earth, Geosci. Model Dev., 7, 2435–2475, https://doi.org/10.5194/gmd-7-2435-2014, 2014.

O'Dowd, C. D., Facchini, M. C., Cavalli, F., Ceburnis, D., Mircea, M., Decesari, S., Fuzzi, S., Young, J. Y., and Putaud, J. P.: Biogenically driven organic contribution to marine aerosol, Nature, 431, 676–680, https://doi.org/10.1038/nature02959, 2004.

O'Dowd, C. D., Langmann, B., Varghese, S., Scannell, C., Ceburnis, D., and Facchini, M. C.: A combined organic-inorganic sea-spray source function, Geophys. Res. Lett., 35, L01801, https://doi.org/10.1029/2007GL030331, 2008.

O'Sullivan, D., Murray, B. J., Ross, J. F., and Webb, M. E.: The adsorption of fungal ice-nucleating proteins on mineral dusts: a terrestrial reservoir of atmospheric ice-nucleating particles, Atmos. Chem. Phys., 16, 7879–7887, https://doi.org/10.5194/acp-16-7879-2016, 2016.

Olivié, D. J. L., van Velthoven, P. F. J., Beljaars, A. C. M., and Kelder, H. M.: Comparison between archived and off-line diagnosed convective mass fluxes in the chemistry transport model TM3, J. Geophys. Res. Atmos., 109, 1–13, https://doi.org/10.1029/2003JD004036, 2004.

Olson, J.: Major World Ecosystem Complexes Ranked by Carbon in Live Vegetation: A Database (NDP-017) (2001 version of original 1985 data). Carbon Dioxide Information Analysis Center (CDIAC), Oak Ridge National Laboratory (ORNL), Oak Ridge, TN (United States), ESS-DI, https://doi.org/10.3334/CDIAC/LUE.NDP017, 1992.

Paytan, A., Cade-Menun, B. J., McLaughlin, K., and Faul, K. L.: Selective phosphorus regeneration of sinking marine particles: evidence from 31P-NMR, Mar. Chem., 82, 55–70, https://doi.org/10.1016/S0304-4203(03)00052-5, 2003.

Peckhaus, A., Kiselev, A., Hiron, T., Ebert, M., and Leisner, T.: A comparative study of K-rich and Na/Ca-rich feldspar ice-nucleating particles in a nanoliter droplet freezing assay, Atmos. Chem. Phys., 16, 11477–11496, https://doi.org/10.5194/acp-16-11477-2016, 2016.

Perlwitz, J. P., Pérez García-Pando, C., and Miller, R. L.: Predicting the mineral composition of dust aerosols – Part

https://doi.org/10.5194/egusphere-2024-952
Preprint. Discussion started: 19 April 2024

1: Representing key processes, Atmos. Chem. Phys., 15, 11593–11627, https://doi.org/10.5194/acp-15-11593-2015, 2015a.

Perlwitz, J. P., Pérez García-Pando, C., and Miller, R. L.: Predicting the mineral composition of dust aerosols – Part 2: Model evaluation and identification of key processes with observations, Atmos. Chem. Phys., 15, 11629–11652, https://doi.org/10.5194/acp-15-11629-2015, 2015b.

Pöschl, U., Martin, S. T., Sinha, B., Chen, Q., Gunthe, S. S., Huffman, J. A., Borrmann, S., Farmer, D. K., Garland, R. M., Helas, G., Jimenez, J. L., King, S. M., Manzi, A., Mikhailov, E., Pauliquevis, T., Petters, M. D., Prenni, A. J., Roldin, P., Rose, D., Schneider, J., Su, H., Zorn, S. R., Artaxo, P., and Andreae, M. O.: Rainforest Aerosols as Biogenic Nuclei of Clouds and Precipitation in the Amazon, Science (80-.)., 329, 1513–1516, https://doi.org/10.1126/science.1191056, 2010.

Prenni, A. J., Petters, M. D., Kreidenweis, S. M., Heald, C. L., Martin, S. T., Artaxo, P., Garland, R. M., Wollny, A. G., and Pöschl, U.: Relative roles of biogenic emissions and Saharan dust as ice nuclei in the Amazon basin, Nat. Geosci., 2, 402–405, https://doi.org/10.1038/ngeo517, 2009.

Pruppacher, H. R., Klett, J. D., and Wang, P. K.: Microphysics of Clouds and Precipitation, Aerosol Sci. Technol., 28, 381–382, https://doi.org/10.1080/02786829808965531, 1998.

Pummer, B. G., Bauer, H., Bernardi, J., Bleicher, S., and Grothe, H.: Suspendable macromolecules are responsible for ice nucleation activity of birch and conifer pollen, Atmos. Chem. Phys., 12, 2541–2550, https://doi.org/10.5194/acp-12-2541-2012, 2012.

Pummer, B. G., Budke, C., Augustin-Bauditz, S., Niedermeier, D., Felgitsch, L., Kampf, C. J., Huber, R. G., Liedl, K. R., Loerting, T., Moschen, T., Schauperl, M., Tollinger, M., Morris, C. E., Wex, H., Grothe, H., Pöschl, U., Koop, T., and Fröhlich-Nowoisky, J.: Ice nucleation by water-soluble macromolecules, Atmos. Chem. Phys., 15, 4077–4091, https://doi.org/10.5194/acp-15-4077-2015, 2015.

Raman, A., Hill, T., Demott, P. J., Singh, B., Zhang, K., Ma, P. L., Wu, M., Wang, H., Alexander, S. P., and Burrows, S. M.: Long-term variability in immersion-mode marine ice-nucleating particles from climate model simulations and observations, Atmos. Chem. Phys., 23, 5735–5762, https://doi.org/10.5194/acp-23-5735-2023, 2023.

Ramelli, F., Henneberger, J., David, R. O., Bühl, J., Radenz, M., Seifert, P., Wieder, J., Lauber, A., Pasquier, J. T., Engelmann, R., Mignani, C., Hervo, M., and Lohmann, U.: Microphysical investigation of the seeder and feeder region of an Alpine mixed-phase cloud, Atmos. Chem. Phys., 21, 6681–6706, https://doi.org/10.5194/acp-21-6681-2021, 2021.

Russell, G. L. and Lerner, J. A.: A New Finite-Differencing Scheme for the Tracer Transport Equation, J. Appl. Meteorol., 20, 1483–1498, https://doi.org/10.1175/1520-0450(1981)020<1483:ANFDSF>2.0.CO;2, 1981.

Sassen, K., DeMott, P. J., Prospero, J. M., and Poellot, M. R.: Saharan dust storms and indirect aerosol effects on clouds: CRYSTAL-FACE results, Geophys. Res. Lett., 30, 1–4, https://doi.org/10.1029/2003GL017371, 2003.

Seinfeld, J. H. and Pandis, S. N.: Atmospheric chemistry and physics : from air pollution to climate change, New York (N.Y.) : Wiley, 1998.

Si, M., Evoy, E., Yun, J., Xi, Y., Hanna, S. J., Chivulescu, A., Rawlings, K., Veber, D., Platt, A., Kunkel, D., Hoor, P., Sharma, S., Richard Leaitch, W., and Bertram, A. K.: Concentrations, composition, and sources of ice-nucleating particles in the Canadian High Arctic during spring 2016, Atmos. Chem. Phys., 19, 3007–3024, https://doi.org/10.5194/acp-19-3007-2019, 2019.

Sorooshian, A., Feingold, G., Lebsock, M. D., Jiang, H., and Stephens, G. L.: On the precipitation susceptibility of clouds to aerosol perturbations, Geophys. Res. Lett., 36, L13803, https://doi.org/10.1029/2009GL038993, 2009.

Spracklen, D. V. and Heald, C. L.: The contribution of fungal spores and bacteria to regional and global aerosol number and ice nucleation immersion freezing rates, Atmos. Chem. Phys., 14, 9051–9059, https://doi.org/10.5194/acp-14-9051-2014, 2014.

Subba, T., Zhang, Y., and Steiner, A. L.: Simulating the Transport and Rupture of Pollen in the Atmosphere, J. Adv. Model. Earth Syst., 15, 1–25, https://doi.org/10.1029/2022MS003329, 2023.

Sullivan, S. C., Hoose, C., Kiselev, A., Leisner, T., and Nenes, A.: Initiation of secondary ice production in clouds,

https://doi.org/10.5194/egusphere-2024-952
Preprint. Discussion started: 19 April 2024

Atmos. Chem. Phys., 18, 1593–1610, https://doi.org/10.5194/acp-18-1593-2018, 2018.

Suski, K. J., Hill, T. C. J., Levin, E. J. T., Miller, A., DeMott, P. J., and Kreidenweis, S. M.: Agricultural harvesting emissions of ice-nucleating particles, Atmos. Chem. Phys., 18, 13755–13771, https://doi.org/10.5194/acp-18-13755-2018, 2018.

Tegen, I., Harrison, S. P., Kohfeld, K., Prentice, I. C., Coe, M., and Heimann, M.: Impact of vegetation and preferential source areas on global dust aerosol: Results from a model study, J. Geophys. Res. Atmos., 107, https://doi.org/10.1029/2001JD000963, 2002.

Tiedtke, M.: A Comprehensive Mass Flux Scheme for Cumulus Parameterization in Large-Scale Models, Mon. Weather Rev., 117, 1779–1800, https://doi.org/10.1175/1520-0493(1989)117<1779:ACMFSF>2.0.CO;2, 1989.

Tobo, Y., Prenni, A. J., Demott, P. J., Huffman, J. A., McCluskey, C. S., Tian, G., Pöhlker, C., Pöschl, U., and Kreidenweis, S. M.: Biological aerosol particles as a key determinant of ice nuclei populations in a forest ecosystem, J. Geophys. Res. Atmos., 118, 10,100-10,110, https://doi.org/10.1002/jgrd.50801, 2013.

Tsigaridis, K. and Kanakidou, M.: Global modelling of secondary organic aerosol in the troposphere: a sensitivity analysis, Atmos. Chem. Phys., 3, 1849–1869, https://doi.org/10.5194/acp-3-1849-2003, 2003.

Tsigaridis, K. and Kanakidou, M.: Secondary organic aerosol importance in the future atmosphere, Atmos. Environ., 41, 4682–4692, https://doi.org/10.1016/j.atmosenv.2007.03.045, 2007.

Tsigaridis, K., Krol, M., Dentener, F. J., Balkanski, Y., Lathière, J., Metzger, S., Hauglustaine, D. A., and Kanakidou, M.: Change in global aerosol composition since preindustrial times, Atmos. Chem. Phys., 6, 5143–5162, https://doi.org/10.5194/acp-6-5143-2006, 2006.

Vali, G., DeMott, P. J., Möhler, O., and Whale, T. F.: Technical Note: A proposal for ice nucleation terminology, Atmos. Chem. Phys., 15, 10263–10270, https://doi.org/10.5194/acp-15-10263-2015, 2015.

Vergara-Temprado, J., Murray, B. J., Wilson, T. W., O'Sullivan, D., Browse, J., Pringle, K. J., Ardon-Dryer, K., Bertram, A. K., Burrows, S. M., Ceburnis, D., DeMott, P. J., Mason, R. H., O'Dowd, C. D., Rinaldi, M., and Carslaw, K. S.: Contribution of feldspar and marine organic aerosols to global ice nucleating particle concentrations, Atmos. Chem. Phys., 17, 3637–3658, https://doi.org/10.5194/acp-17-3637-2017, 2017.

Vergara-Temprado, J., Miltenberger, A. K., Furtado, K., Grosvenor, D. P., Shipway, B. J., Hill, A. A., Wilkinson, J. M., Field, P. R., Murray, B. J., and Carslaw, K. S.: Strong control of Southern Ocean cloud reflectivity by ice-nucleating particles, Proc. Natl. Acad. Sci. U. S. A., 115, 2687–2692, https://doi.org/10.1073/pnas.1721627115, 2018.

Vignati, E., Facchini, M. C., Rinaldi, M., Scannell, C., Ceburnis, D., Sciare, J., Kanakidou, M., Myriokefalitakis, S., Dentener, F., and O'Dowd, C. D.: Global scale emission and distribution of sea-spray aerosol: Sea-salt and organic enrichment, Atmos. Environ., 44, 670–677, https://doi.org/10.1016/j.atmosenv.2009.11.013, 2010.

Wang, X., Deane, G. B., Moore, K. A., Ryder, O. S., Stokes, M. D., Beall, C. M., Collins, D. B., Santander, M. V., Burrows, S. M., Sultana, C. M., and Prather, K. A.: The role of jet and film drops in controlling the mixing state of submicron sea spray aerosol particles., Proc. Natl. Acad. Sci. U. S. A., 114, 6978–6983, https://doi.org/10.1073/pnas.1702420114, 2017.

Wex, H., Demott, P. J., Tobo, Y., Hartmann, S., Rösch, M., Clauss, T., Tomsche, L., Niedermeier, D., and Stratmann, F.: Kaolinite particles as ice nuclei: Learning from the use of different kaolinite samples and different coatings, Atmos. Chem. Phys., 14, 5529–5546, https://doi.org/10.5194/acp-14-5529-2014, 2014.

Whale, T. F., Holden, M. A., Wilson, T. W., O'Sullivan, D., and Murray, B. J.: The enhancement and suppression of immersion mode heterogeneous ice-nucleation by solutes, Chem. Sci., 9, 4142–4151, https://doi.org/10.1039/c7sc05421a, 2018.

Wieder, J., Ihn, N., Mignani, C., Haarig, M., Bühl, J., Seifert, P., Engelmann, R., Ramelli, F., Kanji, Z. A., Lohmann, U., and Henneberger, J.: Retrieving ice-nucleating particle concentration and ice multiplication factors using active remote sensing validated by in situ observations, Atmos. Chem. Phys., 22, 9767–9797, https://doi.org/10.5194/acp-22-9767-2022, 2022.

Wilson, T. W., Ladino, L. A., Alpert, P. A., Breckels, M. N., Brooks, I. M., Browse, J., Burrows, S. M., Carslaw, K.

https://doi.org/10.5194/egusphere-2024-952
Preprint. Discussion started: 19 April 2024

S., Huffman, J. A., Judd, C., Kilthau, W. P., Mason, R. H., McFiggans, G., Miller, L. A., Nájera, J. J., Polishchuk, E., Rae, S., Schiller, C. L., Si, M., Temprado, J. V., Whale, T. F., Wong, J. P. S., Wurl, O., Yakobi-Hancock, J. D., Abbatt, J. P. D., Aller, J. Y., Bertram, A. K., Knopf, D. A., and Murray, B. J.: A marine biogenic source of atmospheric ice-nucleating particles., Nature, 525, 234–8, https://doi.org/10.1038/nature14986, 2015.

Yi, B.: Diverse cloud radiative effects and global surface temperature simulations induced by different ice cloud optical property parameterizations, Sci. Rep., 12, 1–11, https://doi.org/10.1038/s41598-022-14608-w, 2022.

Yin, J., Wang, D., and Guoqing, Z.: An Evaluation of Ice Nuclei Characteristics from the Long-term Measurement Data over North China An Evaluation of Ice Nuclei Characteristics from the Long-term Measurement Data over North China, https://doi.org/10.1007/s13143-012-0020-8, 2012.

Zhang, D., Wang, Z., Heymsfield, A., Fan, J., Liu, D., and Zhao, M.: Quantifying the impact of dust on heterogeneous ice generation in midlevel supercooled stratiform clouds, Geophys. Res. Lett., 39, 1–6, https://doi.org/10.1029/2012GL052831, 2012.

Zhang, H., Zhao, M., Chen, Q., Wang, Q., Zhao, S., Zhou, X., and Peng, J.: Water and ice cloud optical thickness changes and radiative effects in East Asia, J. Quant. Spectrosc. Radiat. Transf., 254, 107213, https://doi.org/10.1016/j.jqsrt.2020.107213, 2020.

Zhao, X., Liu, X., Burrows, S. M., and Shi, Y.: Effects of marine organic aerosols as sources of immersion-mode ice-nucleating particles on high-latitude mixed-phase clouds, Atmos. Chem. Phys., 21, 2305–2327, https://doi.org/10.5194/acp-21-2305-2021, 2021.

Zhou, C., Zelinka, M. D., and Klein, S. A.: Impact of decadal cloud variations on the Earth's energy budget, Nat. Geosci., 9, 871–874, https://doi.org/10.1038/ngeo2828, 2016.

Zolles, T., Burkart, J., Häusler, T., Pummer, B., Hitzenberger, R., and Grothe, H.: Identification of ice nucleation active sites on feldspar dust particles, J. Phys. Chem. A, 119, 2692–2700, https://doi.org/10.1021/jp509839x, 2015.

https://doi.org/10.5194/egusphere-2024-952
Preprint. Discussion started: 19 April 2024

Figures

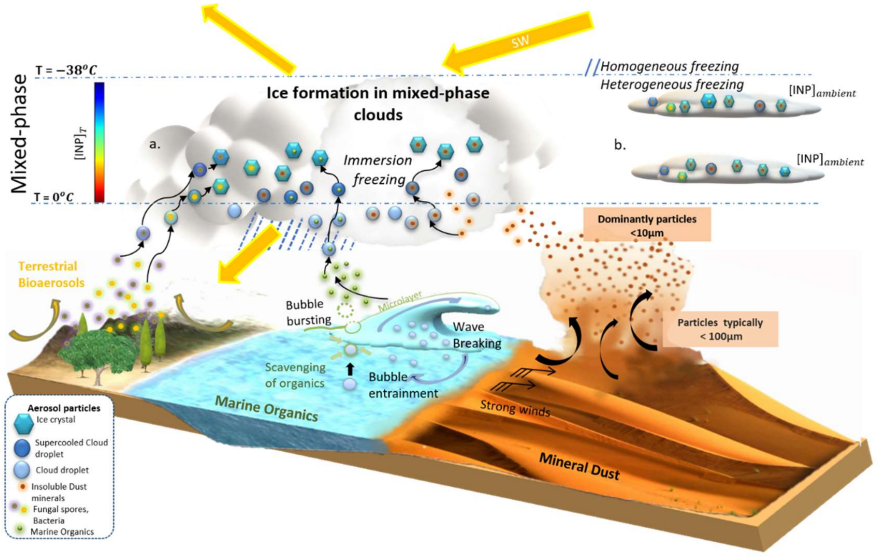

Figure 1: Illustration of the formation of INP from mineral dust, MPOA and PBAP, as well as the two ways in which we display INP concentrations in the present study: $[INP]_{ambient}$ calculated at ambient model temperature relevant to non-deep convective mixed-phase clouds using the ambient temperature in the model temperature level (b.), and $[INP]_T$ calculated at a fixed temperature relevant for vertically extended clouds as deep-convective systems (a.). The figure is based on Chatziparaschos et al. (2023).

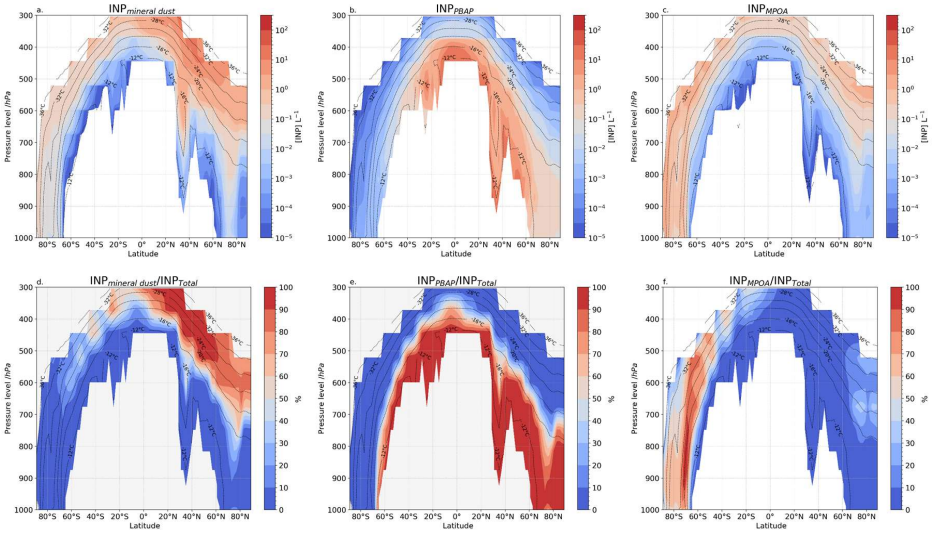

Figure 2: Annual zonal mean profiles of [INP] number concentration calculated by TM4-ECPL for the year 2015 and accounting for (a) mineral dust, (b) fungal spores and bacteria (PBAP) and (c) marine bioaerosols. Panels (d-f) depict the percentage contribution of each species to the total INP concentration. The black contour dashed lines show the annual mean temperature of the model. The colours show (a-c) the INP concentration and (d-f) the percentage contribution of each species to the total INP.

https://doi.org/10.5194/egusphere-2024-952
Preprint. Discussion started: 19 April 2024

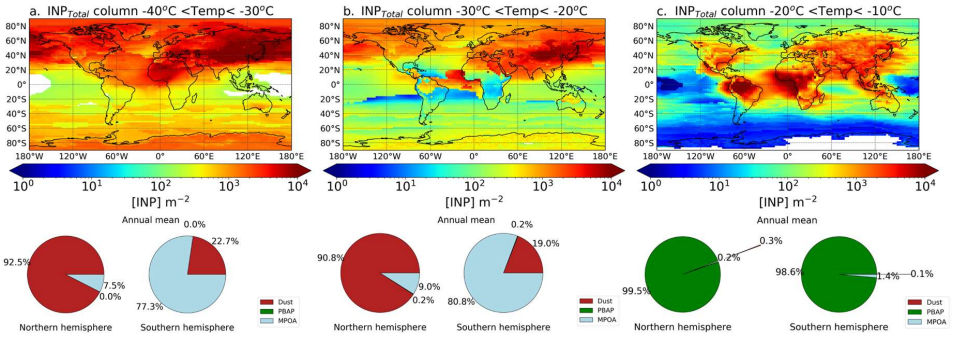

Figure 3: Annual mean INP column concentrations classified by model temperature range between -40 °C to -30 °C (a), -30 °C to -20 °C (b) and -20 °C to -10 °C (c) followed by the respective percentage contributions originated from mineral dust (red), MPOA (light blue) and PBAP (green) in each hemisphere.

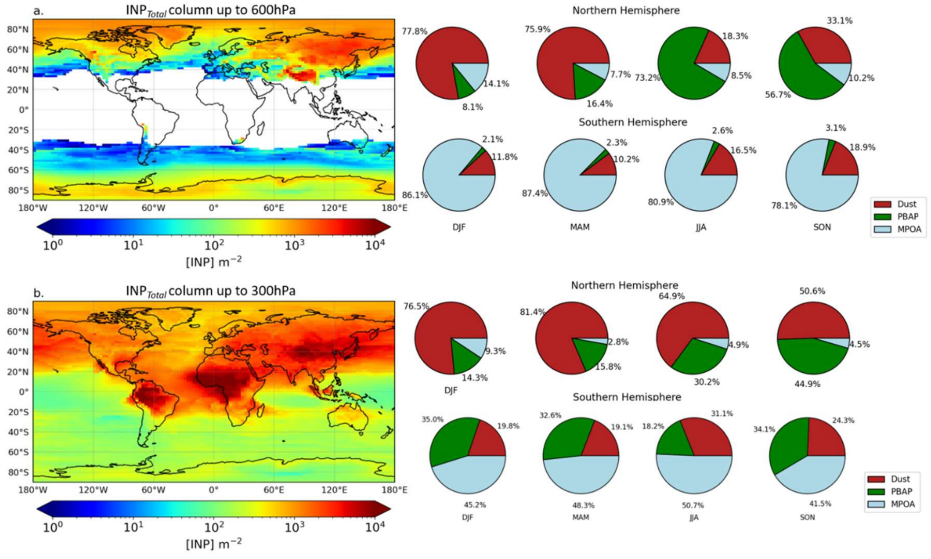

Figure 4: Annual mean INP column concentrations up to 600 hPa (a) and up to 300 hPa (b), and the seasonal percentage contributions originated from mineral dust (red), MPOA (light blue) and PBAP (green) in each hemisphere.

https://doi.org/10.5194/egusphere-2024-952
Preprint. Discussion started: 19 April 2024

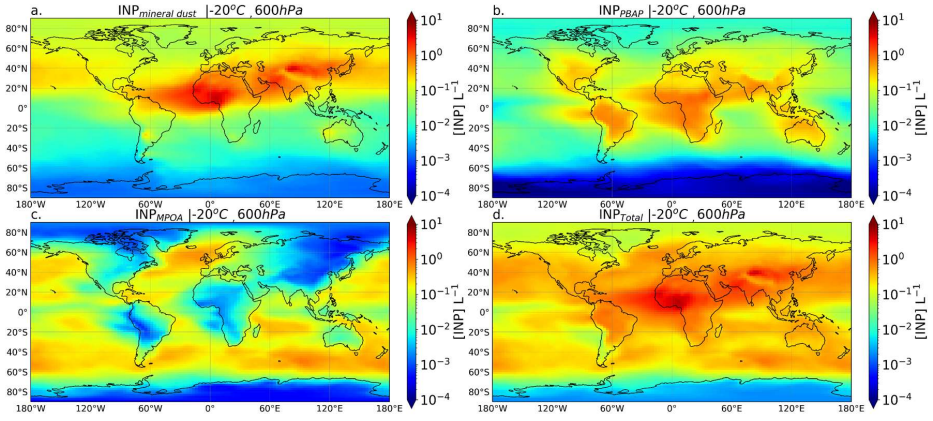

Figure 5. Annual mean distributions calculated by TM4-ECPL for INP number concentrations derived from dust (a), PBAP (b), MPOA (c), and the sum of the aforementioned INP (d) for activation temperature of −20°C, at a pressure level of 600 hPa.

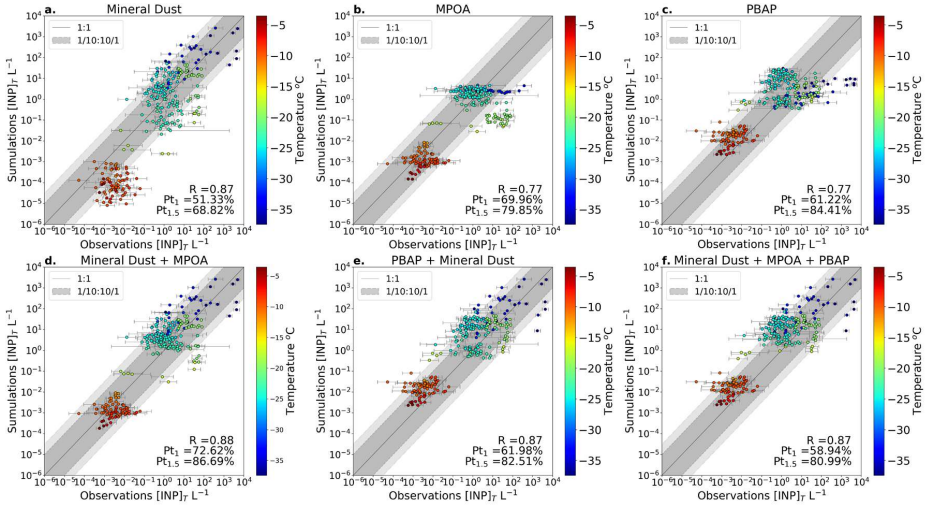

Figure 6. Comparison of INP concentrations calculated at the temperature of the measurements against observations accounting for mineral dust (a), MPOA (b), PBAP (c), mineral dust and MPOA (d), PBAP and mineral dust (e), and mineral dust, MPOA and PBAP (f). The dark grey dashed lines represent one order of magnitude difference between modelled and observed concentrations, and the light-grey dashed lines depict 1.5 orders of magnitude. The simulated values correspond to monthly mean concentrations, and the error bars correspond to the error of the observed monthly mean INP values. The color bars show the corresponding instrument temperature of the measurement in Celsius (a-f). Pt1 and Pt1.5 are the percentages of data points reproduced by the model within an order of magnitude and 1.5 orders of magnitude, respectively. R is the correlation coefficient, which is calculated with the logarithm of the values.